RDU 140118

DISSIMILAR METAL JOINING OF ALUMINIUM AND MAGNESIUM ALLOY BY GAS METAL ARC SPOT WELDING TECHNIQUE

MAHADZIR BIN ISHAK

RESEARCH VOTE NO:
RDU140118

Faculty of Mechanical Engineering
Universiti Malaysia Pahang

2017

ABSTRACT

DISSIMILAR METAL JOINING OF ALUMINIUM AND MAGNESIUM ALLOY BY GAS METAL ARC SPOT WELDING TECHNIQUE

(keywords; aluminium, magnesium, dissimilar welding, laser, FSW, MIG, plug weld)

Innovative welding technique for joining aluminum and magnesium alloys in automobile, aviation, aerospace and marine industries would achieve weight reduction, high specific strength as well as increase fuel efficiency and reduce environmental pollution. Friction stir welding (FSW) is capable of joining magnesium alloys without melting, and thus, it can eliminate problems related to solidification. Thin sheet AZ31B finds its application in automotive, aviation and also electronic devices parts such as computer casing and thin plate part in smartphone. In joining thin sheet AZ31B, laser welding is promising the best joining method compared to arc and solid state welding in producing small weldments.Magnesium alloy AZ31 was successfully welded by using friction stir welding. Shoulder to pin diameter ratio give effect to the mechanical properties and microstructural properties of AZ31 FSW. The optimum shoulder to pin ratio shows higher tensile strength with fine and equiaxed grain size that indicate higher hardness.The fine grain produced higher hardness values compared to the coarser grain with a value of 77 Hv for the optimized sample. Optimized sample has 80.5 MPa of tensile shear strength and fracture load of 800 N which could be applied in replacing Al and steel especially for the electronic parts since the strength was acceptable for a thin product.

However, poor mechanical properties of welding joint between aluminum and magnesium alloys due to the formation of Al_mMg_n type brittle intermetallic compounds is the main barrier for extensive uses of these two alloys especially in transportation sectors.The results revealed that more significant mechanical properties were achieved with stainless steel filler compared to aluminum filler. The maximum yield strength, ultimate tensile strength and fracture toughness were 203.09 MPa, 249.33 MPa and 27.49 MPa√m respectively with steel filler; and 176.30 MPa, 226.28 MPa and 20.22 MPa√m respectively with aluminum filler.The output of this research exhibited very significant mechanical properties of the joint that can facilitate the extensive uses of A7075-T651 and AZ31B alloys in mass production of light weight vehicle structures in transportation industries.

Key researchers **:** Mahadzir bin Ishak
Siti Rabiatull Aisha binti Idris
Aiman bin Mohd Halil
Wan Azhar bin Wan Yusoff

E-mail : *mahadzir@ump.edu.my*
Tel. No. : 09 424 6235

Vote No. : RDU140118

ABSTRAK

Teknik kimpalan yang inovatif perlu untuk menggabungkan aluminium dan magnesium aloi untuk diaplikasikan dalam pembuatan otomobil, kapal terbang, aero-angkasa dan industri marin. Selain itu, ia akan dapat menyumbang kearah pengurangan berat, meningkatkan kekuatan khusus (spesific strength) bahan serta peningkatan kecekapan bahan api dan mengurangkan pencemaran alam sekitar. Kimpalan geseran kacau (FSW) mampu menghasilkan aloi magnesium tanpa lebur, dan dengan itu, ia boleh menghapuskan masalah yang berkaitan dengan pemejalan. AZ31B berketebalan nipis digunakan dalam aplikasi automotif, penerbangan dan bahagian peranti elektronik seperti selongsong komputer dan kepingan nipis di dalam telefon pintar. AZ31 aloi magnesium telah berjaya dikimpal dengan menggunakan kimpalan geseran kacau. Nisbah bahu kepada pin diameter memberi kesan kepada sifat-sifat mekanikal dan sifat-sifat mikrostruktur kimpalan geseran kacau AZ31. Nisbah optimum bahu kepada pin menunjukkan kekuatan tegangan yang lebih tinggi dengan saiz butiran *equiaxed* dan halus dan menunjukkan kekerasan yang lebih tinggi. Biji halus menghasilkan nilai kekerasan yang lebih tinggi berbanding dengan bijirin kasar dengan nilai 77 Hv untuk sampel yang dioptimumkan. Sampel yang dioptimumkan mempunyai 80.5 MPa kekuatan ricih tegangan dan beban patah 800 N yang boleh digunakan untuk menggantikan Al dan keluli terutamanya untuk bahagian-bahagian elektronik kerana kekuatannya boleh diterima untuk produk nipis.

Walau bagaimanapun, kelemahan sifat mekanikal dalam gabungan kimpalan di antara aluminium dan magnesium aloi disebabkan oleh pembentukan Al_mMg_n iaitu sejenis sebatian antara logam yang rapuh menjadi halangan utama untuk menggunakan kedua-dua aloi ini dalam sektor pengangkutan.Keputusan mendedahkan bahawa sifat mekanik lebih ketara dicapai menggunakan pengisi keluli berbanding dengan pengisi aluminium. Kekuatan alah maksimum, kekuatan tegangan muktamad dan keliatan patah adalah 203,09 MPa, 249.33 Mpa dan 27.49 MPa√m masing-masing dengan pengisi keluli; dan 176.30 MPa, 226.28 MPa dan 20.22 MPa√m masing-masing dengan pengisi aluminium. Hasil kajian ini boleh menawarkan ciri-ciri sifat mekanikal gabungan kimpalan yang bererti. Kajian ini boleh mempermudahkan penggunaan A7075-T651 dan AZ31B aloi yang lebih meluas dalam pengeluaran massa struktur kenderaan ringan dalam industri pengangkutan.

TABLE OF CONTENTS

LIST OF TABLES

LIST OF FIGURES

LIST OF ADDITIONAL RELATED PUBLICATIONS

CHAPTER 1

INTRODUCTION

1.1 INTRODUCTION

This chapter introduces the background related to the dissimilar welding between aluminium (Al) and magnesium (Mg) alloys which consists of different element compositions. Through its core problems, which is hard to join those two materials due to its different alloying elements iniated us to solve this problems which then could apply this product of dissimilar welding of Al and Mg alloy to the industries in promising light weight structures with high rate of corrosion resistance. Finally, the main objectives and scopes of the project will be presented.

1.2 BACKGROUND

Metal can be joined by using several methods. In general, methods that can be used in joining metal are soldering, brazing and welding. Brazing is a process in which filler metals are melted and distributed between multiple solid metal components after heated to a proper temperature. The filler metal must have a melting point below 448.89° C but below the melting point of the based metal [1]. No melting of based material occurs during brazing. Friction stir welding is a joining process that involves solid state joining technique that has expended rapidly since its development in 1991 [2,3]. Thin sheet metal such as AZ31B magnesium alloy usually produced by using hot-rolled sheet of wire-electrode cutting method in order to enhanced its mechanical properties [4]. The application of thin sheet metals usually found in automotive, aviation, and electronic devices as an alternative of reducing weight [5]. Application of laser in material processing is increasing since it was introduced from 1960 [6].

However, Both Al and Mg alloys have many attractive physical, mechanical and chemical properties like light weight, very good thermal and electrical conductivity, high specific strength, high stiffness, good formability, high durability, recyclability, excellent corrosion resistance, low cost maintenance, high recovery potential. Infact,

Mg is the lightest (around two-thirds of Al and one fifth of steel) of all structural metals on earth with some other properties like good castability, workability and electromagnetic shielding capability [7-10]. Currently, the welding technology between Al and Mg alloys has been an important research field in transportation industries. The intersection of modern industrial materials has also made the welding technology of Al and Mg alloys urgently [11]. The welding joint is also one of the most important factors affecting the life span, safety, endurance and quality of the structures [12]. Thus, for extensive practical applications of Al and Mg alloys; efficient and reliabile welding technologies should be established in addition to consider issues such as alloy design, microstructure control, plastic forming and surface treatment.

1.3 PROBLEM STATEMENT

Magnesium alloys possesses low density, excellent specific stiffness, good strength and recycle ability which is beneficial in producing lightweight structural parts in automotive and aerospace industries. Magnesium alloys can be conventional fusion welding causes large coefficient of expansion of Mg alloy which can cause large deformation/distortion of the welded metal, so FSW is an alternative method to overcome the disadvantages since it can be joined using wide variety of process. A few past researchers have studied about welding of thin sheet AZ31B magnesium alloy. Laser has been a trending up method for past few years to weld AZ31B sheets since laser was able to produce lower heat input compared to conventional arc welding method. A complicated method such as ultrasonic spot welding which require high frequency vibrator to join the part without melting the base metal [13]. Longer welding time and higher amplitude level needed to achieve higher fracture load. A single fillet lap joint of 0.3 mm thick AZ31B has been welded using pulse wave (PW) mode of Nd:YAG laser with silver nanoparticle [14].

However, a variety of attempts have been taken so far to find out the best method to join Al to Mg alloys such as arc, metal inert gas (MIG), tungsten inert gas (TIG), friction stir welding (FSW), diffusion, laser, laser-TIG hybrid, laser and electron beam welding [12,15]. Moreover, the flexibility of FSW is poor, diffusion bonding is less efficient and needs to be put in a vacuum chamber. Laser and hybrid laser-TIG welding need expensive equipment and complex welding procedures. Therfore, these methods are some what limited in applications. Meanwhile; TIG, MIG, GMA, laser and other conventional fusion welding inevitably make fusion zone to generate a thick

Al_mMg_n IMCs layer, which leads to the formation of cracks seriously affecting the mechanical and metallurgical properties of the joint [11,15]. Additionally, a few research was reported so far to investigate the fracture tougness (FT) of the joints betwen any Al to Mg alloys. But, FT is a very important mechanical property that describes the impact resistance of materials and welding joints. Therefore; from the above discussions, it can be stated that most of the fusion and non fusion welding methods for joining Al to Mg alloys have drawbacks mainly because of the formation of Al_mMg_n IMCs. Considering these drawbacks and taking the simple conventional arc welding method into account, the principal technical challenge was to combine Al and Mg alloys by a reliable joining technique of GMA welding for their extensive structural applications [16].

1.4 OBJECTIVES

The core objectives of the study are

i. to investigate the weldability of magnesium alloy using friction stir welding and low power fiber laser welding on mechanical and microstructure properties.
ii. to develop welding joint of dissimilar A7075-T651 and AZ31B alloys using ER308L-Si stainless steel and ER5356 aluminum filler wires by new technique of gas metal arc lap plug welding method.
iii. to investigate weldability, effects of welding parameters on ultimate tensile strength and fracture toughness, and develop mathematical models for the dissimilar welding between Al and Mg.

1.5 SCOPE OF STUDY

i. the materials used in this studies are AA6061, AA7075, and AZ31B with different thicknesses based on different welding method.
ii. Develop a Box-Behnken design of experiment for welding of A7075-T651 and AZ31B alloys
iii. Conduct a new technique of gas metal arc lap plug welding method to join dissimilar A7075-T651 and AZ31B alloys using ER308L-Si stainless steel and ER5356 aluminum filler wires.
iv. The mechanical testing of the weld joints is conducted for tensile and hardness properties

v. Studying fracture surface morphology after mechanical testing and analyzing chemical composition at welding joints by scanning electron microscope and energy dispersive spectroscopy.

1.6 REFERENCE

[1] Weisman, C., & Kearns, W. H. (2010). Welding processes - Arc and gas welding and cutting, brazing, and soldering. *Welding Handbook*, *2*(7).

[2] Arbegast, W. J. (2003). Friction Stir Joining : Characteristic Defects. *Advanced Materials Processing Center MET*, *6*(October), 1–30.

[3] Burford, D., Widener, C., & Tweedy, B. (2006). Advances in Friction Stir Welding for aerospace applications. *6th AIAA Aviation Technology, Integration and Operations Conference (ATIO)*, *6*(14), 3–7. http://doi.org/10.2514/6.2006-7730.

[4] Pan, H., Ren, Y., Fu, H., Zhao, H., Wang, L., Meng, X., and Qin, G. (2016). Recent developments in rare-earth free wrought magnesium alloys having high strength: A review. *Journal of Alloys and Compounds*, *663*, pp.321-331.

[5] Simoncini, M., and Forcellese, A. (2012). Effect of the welding parameters and tool configuration on micro- and macro-mechanical properties of similar and dissimilar FSWed joints in AA5754 and AZ31 thin sheets. *Materials & Design*, *41*, pp.50-60.

[6] Odabaşı, A., Ünlü, N., Göller, G., and Eruslu, M. N. (2010). A Study on Laser Beam Welding (LBW) Technique: Effect of Heat Input on the Microstructural Evolution of Superalloy Inconel 718. *Metallurgical and Materials Transactions A*, *41*(9), pp.2357-2365.

[7] Casalino, G. 2007. Statistical analysis of MIG-laser CO_2 hybrid welding of Al–Mg alloy. *Journal of Materials Processing Technology.***191:**106-110.

[8] Chen, Y. and Nakata, K. 2008. Friction stir lap joining aluminum and magnesium alloys. *Scripta Materialia*. **58:**433-436.

[9] Chang, W. S., Rajesh, S. R., Chun, C. K. and Kim, H. J. 2011. Microstructure and mechanical properties of hybrid laser-friction stir welding between AA6061-T6 Al alloy and AZ31 Mg alloy. *Journal of Materials Science& Technology.* **27:**199-204.

[10] Gourier-Fréry, C. and Fréry, N. 2004. Aluminium. *EMC-Toxicologie-Pathologie.* **1:** 79-9

[11] Shang, J., Wang, K. H., Zhou, Q., Zhang, D. K., Huang, J. and Ge, J. Q. 2012. Effect of joining temperature on microstructure and properties of diffusion bonded Mg/Al joints. *Transactions of Nonferrous Metals Society of China.***22:** 1961-1966.

[12] Hayat, F. 2011. The effects of the welding current on heat input, nugget geometry, and the mechanical and fractural properties of resistance spot welding on Mg/Al dissimilar materials. *Materials & Design.* **32:** 2476-2484.

[13] Michael, D. L., and Shin, H. S. (2017). Weldability assessment of Mg alloy (AZ31B) sheets by an ultrasonic spot welding method. *Journal of Materials Processing Technology*, *243*, pp.1-8.

[14] Ishak, M., Yamasaki, K., and Maekawa, K. (2012). Laser Welding of Thin Sheet Magnesium Alloys. In I. Tech (Ed.), *Nd:YAG Lasers* (Vol. 2016, pp. 135-157): In Tech Open Access.

[15] Zhang, H. T. and Song, J. Q. 2011. Microstructural evolution of aluminum/magnesium lap joints welded using MIG process with zinc foil as an interlayer. *Materials Letters.***65:** 3292-3294.

[16] Liu, F., Ren, D. and Liu, L. 2013. Effect of Al foils interlayer on microstructures and mechanical properties of Mg–Al butt joints welded by gas tungsten arc welding filling with Zn filler metal. *Materials & Design*. **46:**419-425.

CHAPTER2

TECHNICAL PAPER #1

Title:- A study on bead on plate welding of AA7075 by low power fiber laser
(Journal of Mechanical Engineering and Science (2016) 012066
doi:10.15282/jmes.10.2.2016.12.0196 – Scopus Indexed)

2.1 ABSTRACT

Laser welding promising the best method to produce higher strength of aluminium joints compared to conventional arc welding process. Arc welding usually produce large heat affected zone (HAZ) which leads to lower joint strength on aluminium alloys. AA7075 aluminium alloy has many advantages due to its light weight, low density, high corrosion resistance, and high strength alloys compared to steel. This paper presents about the weld feasibility studies on AA7075 surface by using low power fiber laser with two different modes; continuous (CW) and pulse (PW) wave mode. The intention of this research work is to investigate the effect of laser welding modes with different focal position on penetration depth, type of weld penetration, and microstructure of bead on plate welded AA 7075 by using low power fiber laser. Bead on plate (BOP) welding was carried out by heating the surface of AA7075 with thicknesses of 2 mm using both CW and PW modes with focal length ranges from 60 to 200 mm. 90 % power was used for both welding mode with same welding speed of 2 mm/s. The macrostructure of welded line were captured using an optical microscope and beam width and penetration was measured. Smallest bead with was observed at focal length of 120 mm with 570 µm diameter. Pulse wave (PW) welding with keyhole profile produced optimum penetration depth which is approximately 1.0 mm. However, continuous mode (CW) welding could produce 0.153 mm penetration depth. To conclude, AA 7075 could be joint using low power fiber laser welding method since half weld penetration with keyhole profile was produced. For a better weld joint with fewer occurrences of defects, shielding gas and incident angle of laser beam could be applied.

2.2 INTRODUCTION

Joining process could be classified in different ways such as mechanical and welding joining. In joining aluminium alloys, conventional arc welding such as Metal Inert Gas (MIG), Tungsten Inert Gas (TIG) and Resistance Spot Weld (RSW) and solid state welding such as Friction Stir Welding (FSW) were used [1-4]. As new development in welding technology, laser welding has been introduced into the industrial world. There were several typical types of lasers used in industries such as Diode, Neodymium-doped: Yttrium Aluminium Garnet (Nd:YAG), Carbon Dioxide (CO_2), and fiber laser. However, fiber laser was observed to be the finest laser type to be applied in welding industry [5]. Fiber laser welding usually was selected due to its low cost maintenance compared to other solid state laser and CO_2 laser [6]. Furthermore, it could reduce cost by using low power fiber laser machine.

The weldability of aluminium alloys in terms of weld penetration which welded by low power fiber laser can be the significance of this study. In addition, this method could replace conventional arc welding since there is no filler metal used which can affect its density. Many researches used high power laser with continuous wave mode to produce weld joint which contributes to high costing includes the maintenances although to weld metal with thicknesses of 2 mm [7-10]. From a previous researcher, a 10kW fiber laser was used to weld 1XXX , 5XXX, 6XXX, and 7XXX series of aluminium alloys with thicknesses of 10 mm [27]. Nd:YAG laser with maximum 2200 Watt power and fiber laser with maximum power of 4000 Watt were used to weld similar joint of AA 7075 [28, 29]. In this research, we used a low power fiber laser which has maximum average power as low as 200 Watt. Laser welding of aluminium alloys was difficult due to their high reflectivity and heat conductivity compared to the ferrous metal [8]. However, laser welding can form a keyhole penetration profile which the heat affected zone (HAZ) will be smaller and can produce a strong weld joint once it can weld the aluminium alloys.

Aluminium alloys has less density which is 1/3 than that of steel and it has strong mechanical properties. AA7075 aluminium alloys had been chosen in this study since it was less study welded by fiber laser welding method and its application remain obscure. The 7000 series itself is a typical heat-treated alloys which can be categorized into high strength Al-Mg-Mg-Cu type represented by AA7050 and AA7075 where the principle added elements used are Al-Zn-Mg [14]. Focus point play important role since

it can affect the peak power density of laser, which measured by a beam profiler [11]. Spot diameter contains the energy of laser light, which is equivalent to the Gaussian distribution ($1/e^2$) [8]. This paper reports the effects of welding mode, pulse and continuous on the penetration depth, type of penetration, and microstructure of BOP welded AA7075 using low power fiber laser as the feasibility study on welding aluminium alloys.

2.3 EXPERIMENTAL SET UP

2.3.1 Experimental Procedure

AA7075 was prepared by dimension of 100 mm x 100 mm with 2 mm thickness using shearing cutting machine. The chemical composition of AA7075 parent metal was checked using spectrometer and the composition were listed in Table 2.1.

Table 2.1. Chemical composition of AA7075.

Elements	Al	Zn	Mg	Cu	Fe	Si	Mn
Compositions (wt.%)	89.8	5.58	2.28	1.6	0.27	0.07	0.02

Ytterbium Laser Machine-Quasi Continuous Wave (YLM-QCW) fiber laser machine with wavelength ranged at 1.0 µm was used. The maximum average power is 200 Watt with peak power of 2 kW for pulse mode (PW) and continuous mode (CW). Bead on plate welding was carried out using both welding modes. The angle of irradiation is 0°. Weld width was measured from sample surface for all of BOP welded line. Welded sample then was cut using cut-off machine and hot mounted to produce the welded cross-section parts.

The welded sample was then prepared through grinding, polishing and etching process. Etching process was very important in order to reveal microstructure of AA7075. Keller's Reagent solution was used for the etching process and its composition is shown in Table 2.2. Penetration depth was measured from the welded cross section and the microstructure was observed by optical microscope (OM). From the metallographic observation, the microstructure behaviour of welded sample will be analysed.

Table 2.2. Keller's reagent composition.

Chemical element	Volume (ml)
Water (H_2O)	94
Nitric Acid (HNO_3)	5
Hydrochloric Acid (HCl)	3
Hydrofluoric Acid (Hf)	2

2.3.2 Experimental Design

In this experimental study, both PW and CW modes were selected for the fiber laser. The parameters for this laser such as power percentage (W), pulse width (ms), pulse repetition rate (Hz), and welding speed (mm/s) was remain constant. The variable parameter is the focal length (mm). Welding configuration was shown in Fig. 2.1. From Fig. 2.1, the focal length datum is measured from the sample surface to the protective mirror. Table 2.3 presents the selective parameter to conduct the BOP welding using low power fiber laser welding.

Fig. 2.2 shows the method to analyse the weld width on the welded AA7075 surface and the weld penetration depth. The smallest weld width will be concluded as the focus point. The highest depth of penetration will be concluded as the optimum depth at the optimum focal position. Welded samples were prepared through grinding, polishing, and etching process to reveal the microstructure. Microstructures for both welded samples using CW and PW modes were observed and analysed in term of grain sizes, grain boundaries, and penetration produced.

Table 2.3. Bead-on-Plate laser welding parameter.

Parameter	**Pulse Mode (PW)**	**Continuous Mode (CW)**
Power (Watt)	1800 W (90%)	180 W (90%)
Welding Speed (mm/s)	2mm/s	
Pulse Width (ms)	1 ms	-
Pulse Repetition Rate (Hz), PRR	20 Hz	-
Focal Length (mm), F	60 mm – 200 mm	

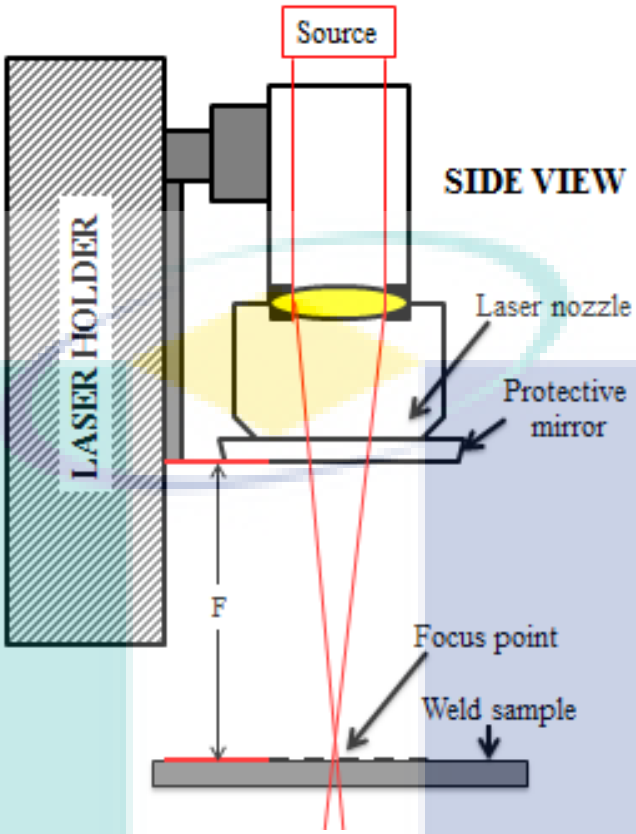

Fig, 2.1. Fiber laser BOP welding setup.

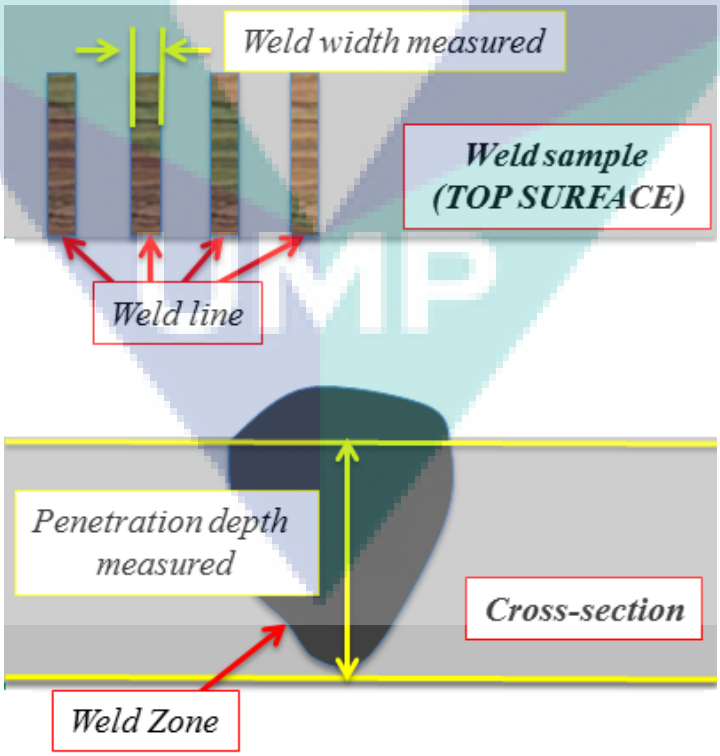

Fig. 2.2. Weld width and depth of penetration analysis.

2.4 RESULTS AND DISCUSSION

2.4.1 Weld Width Analysis and Penetration Depth

Fifteen weld lines had been made for both welding mode. Fig. 2.3 and Fig. 2.4 show the images of the welded line produced from the BOP laser welding for PW and CW mode, respectively. The measurement results of the weld width and depth of penetration for both welding condition was tabulated in Table 2.4. The penetration depth was measured from the sample cross-section obtained from the optical microscope. From Fig. 2.3, it was observed that at focal length, F= 100 mm, good weld appearance produced compared to weld produced at focal length ranged from 110 mm to 140 mm. This is due to the higher energy absorption during PW mode welding as the focal length achieved the focus point on the metal surface [15]. It was shown that starting from F = 150 mm weld line became unclear and no weld line observed when focal length higher than 180 mm since laser beam already defocused at these focal lengths.

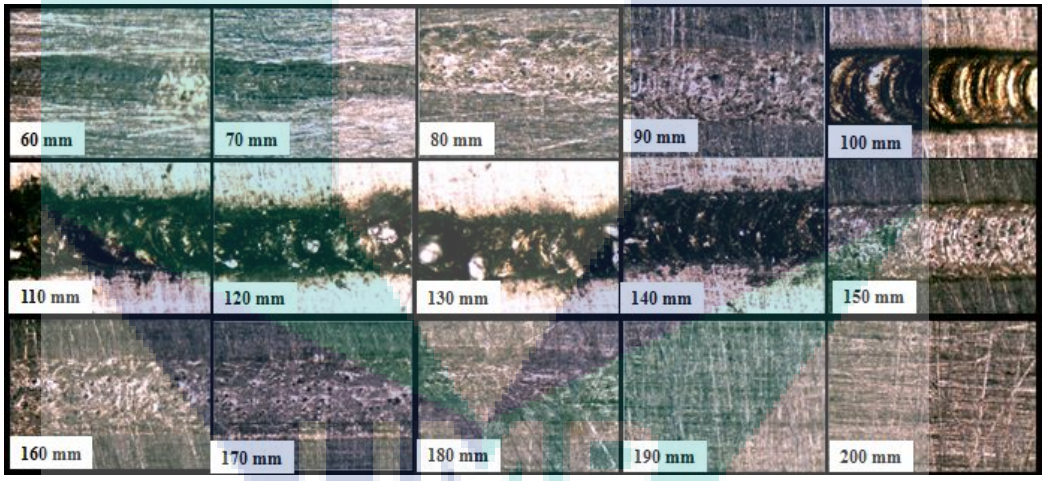

Fig. 2.3. Weld line produced on sample surface (PW) with different focal length.

From Fig. 2.4, it was found that the weld line cannot be obtained at F=150 mm and above using CW welding mode compared to the PW welding mode. This is due to the laser power produced by PW was greater than the power produced by CW since PW have its high peak power at 1.8 kW [16]. From Table 2.4, it was found that the smallest weld width (bead width) measured was obtained at the focal length, F=120 mm for both welding mode with 570 µm and 417 µm for PW and CW mode, respectively. Both welding mode produce different weld width. This is due to the different values of laser power which produce different energy. As shown in Table 2.4, the largest weld with was measured at focal length 180 mm with 785 µm with PW welding mode. Weld line

was none observed at focal length higher than 190 mm and 150 mm for PW and CW, respectively. It was observed as the higher the focal length from the focus point, the laser beams were defocused due to larger laser beam width produced. This situation was also same for the focal length below than 60 mm. For PW mode, pulsed energy plays an important role where the power intensity produced was higher compared to CW mode. This is because of CW mode does not have peak power since it only could produces average laser power during welding process. It was concluded that the focus point of the laser machine on AA 7075 surface was at F=120 mm.

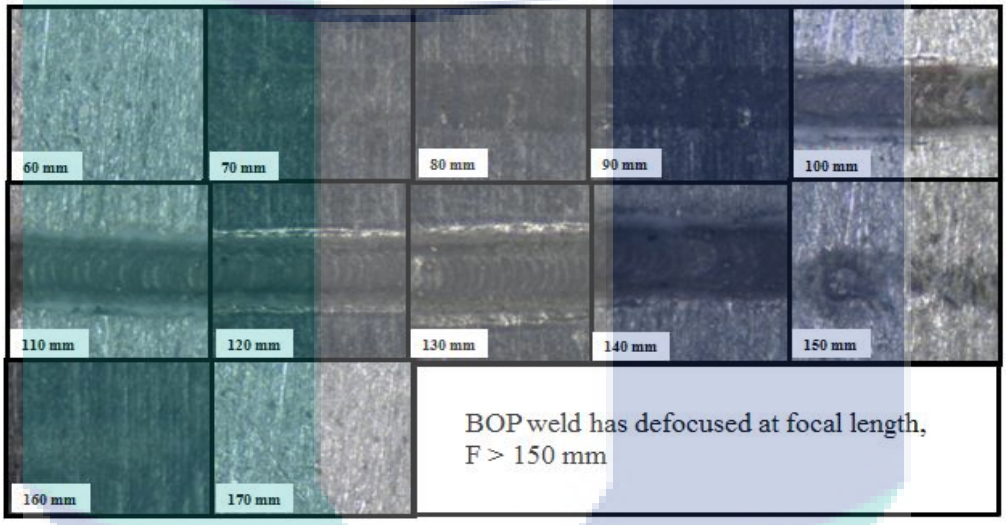

Fig. 2.4. Weld line produced on sample surface (CW) with different focal length.

Table 2.4. Weld width and penetration depth results.

Focal Length (mm)	Weld Width (µm)		Penetration depth (mm)	
	PW Mode	CW Mode	PW Mode	CW Mode
60	617	defocussed	0.030	defocussed
70	626	454	0.040	Non-observed
80	660	484	0.120	0.061
90	699	516	0.130	0.111
100	703	547	0.134	0.173
110	727	478	0.450	0.140
120	570	417	0.990	0.153
130	589	492	0.970	Non-observed
140	687	523	0.230	Non-observed
150	668	defocussed	0.140	defocussed
160	734	defocussed	0.100	defocussed
170	832	defocussed	0.040	defocussed
180	785	defocussed	0.050	defocussed
190	defocussed	defocussed	0.007	defocussed
200	defocussed	defocussed	0.012	defocussed

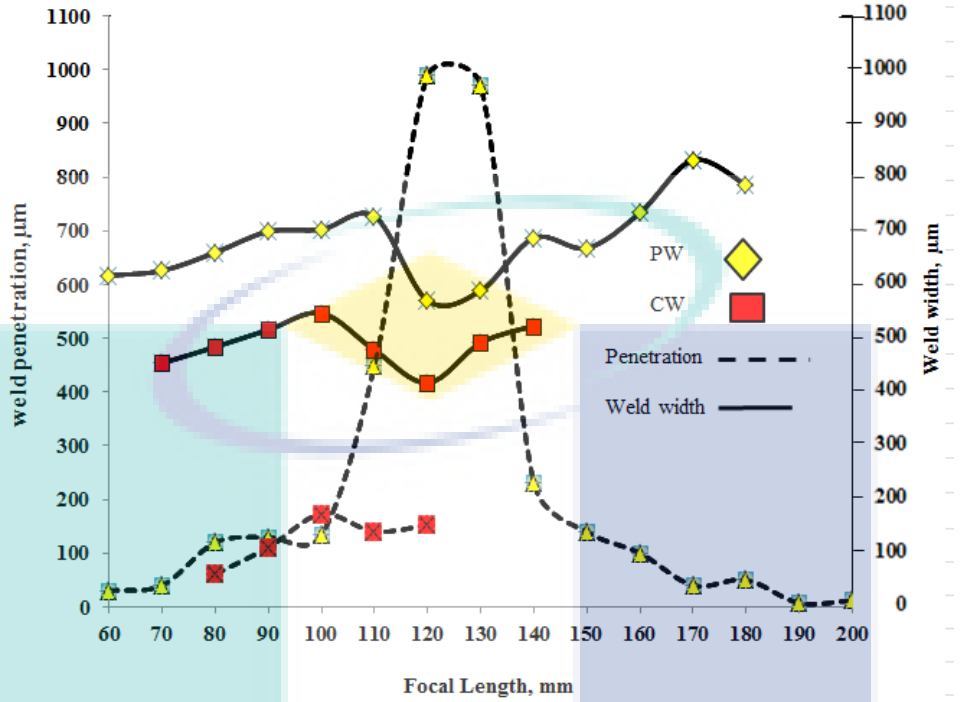

Fig. 2.5. Weld width/weld penetration vs focal length.

Figure 2.5 shows the graph of weld width and depth of penetration versus focal length. From the graph, it was clearly observed that both welding modes produced focus position at the same focal length, F=120 mm. It was proved that the laser beam has the focus point at focal length of 120mm due to the smallest beam diameter produced for both welding mode. From the result, it was observed that PW mode produced highest depth of penetration at the focus point, F with 0.99 mm or half of AA7075 sample compared to CW mode, which only produced 0.173 mm as the highest at F=100 mm.

This is due to the differences in the laser power since PW can produce peak power of 2.0 kW compared to CW, which only produces maximum average power of 200 W. Higher laser power can produce a better penetration due to higher heat input and higher efficiency to make a weld joint with keyhole profile. In addition, PW has different pulsed energy will produce different weld penetration as pulsed laser is pumped at high intensity for short period of time. This is due to the different power density produced to the metal [17]. PW mode also was proved to be a better welding mode where it reduces the porosity with higher weld penetration with smaller grain size produced in weld zone compared to CW [16].

2.4.2 Microstructure analysis

After the BOP laser welding process, the cross section of the welded samples selected from the optimum depth for both welding modes was compared as shown in Fig. 2.6. It was found that PW produced a narrow and deep penetration (keyhole profile) compared to the CW, which only could produce wider weld zone and low penetration depth (conduction profile). From Fig. 2.6 (a), it was observed that the keyhole profile was produced at 0.99 mm depth, which is half of the sample thickness, 2 mm. However, underfill presents as the defects due to there is no shielding gas used in this experiment, where it could not protect the molten pool during the welding process. Keyhole presents when the vapour plume during laser welding process open the keyhole in the molten pool in short time period [34].

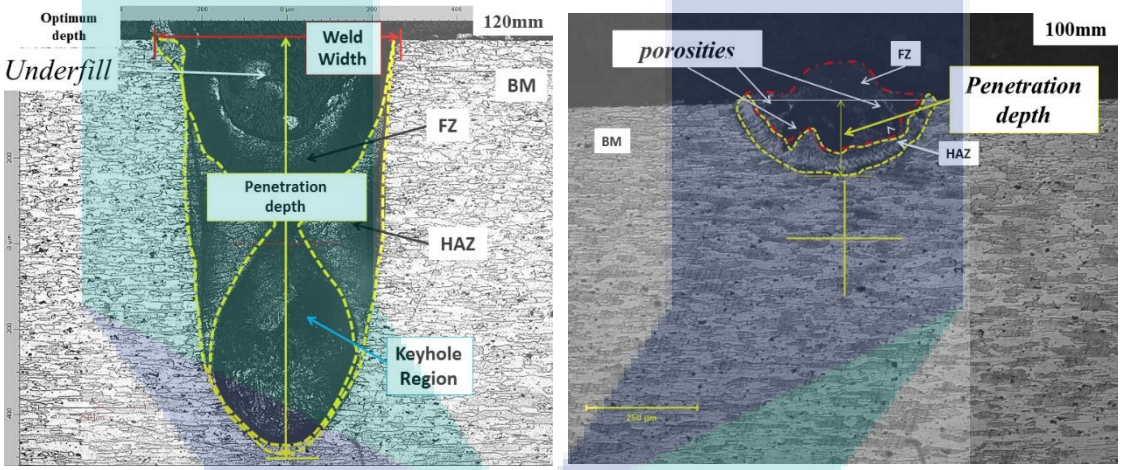

Fig. 2.6. AA7075 BOP laser welded (a) PW (b) CW (10 x magnifications).

Fig. 2.6 (b) shows that the CW produced conduction profile with 0.173 mm of penetration depth. It was found that porosity occurred at the welded zone of sample welded with CW mode, which also due to no shielding gas used. From the microstructure analysis, it was observed that PW welding mode could produces a good weld joint compared to the CW mode in term of weld seam profile, which can contributes to a higher welding joint. With low fibre laser welding machine, half depth of penetration could be achieved for 2 mm thickness of aluminium alloys. Double V-groove welding method could be selected and it can produces stronger weld joint compared to one side penetration for 2 mm thickness of AA7075.

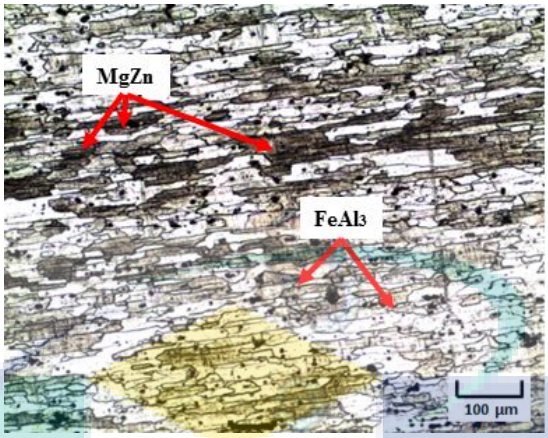

Fig. 2.7. AA7075 base metal (10 x magnifications).

Microstructure for base metal AA7075 shows spheroidal particles of black precipitate MgZn with the light grey of $FeAl_3$ particles [35] as shown in Fig. 2.7, which present in aluminium solid solution and it was observed that the grains elongated horizontally in one direction. It was observed that the element presented in the base metal was proved to be Al, Mg, and Zn element with a small amount of Fe element

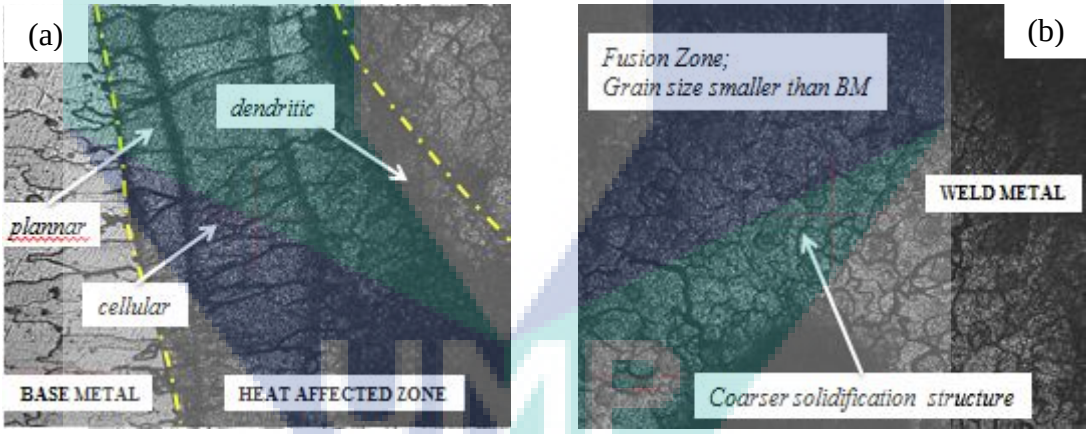

Fig. 2.8. Microstructure of sample welded by PW (keyhole) at (a) PMZ (b) Weld zone.

The best weld result was selected to discuss about the microstructure. Fig. 2.8 (a) shows the microstructure changing from the base metal to weld metal through the partially melted zone (PMZ). The elongated grain structure starts changing to planar grain structure at the HAZ transition line because it was affected by heat from laser source and it turns into cellular grain structure at the centre of HAZ [20]. Dendritic grain structure was observed at the transition line between HAZ and weld zone due to the high amount of heat produce [21]. The hardness at HAZ was lower compared to the

BM as it normally fractured at this point. From Fig. 2.8 (b), it was found that coarser dendritic grain structure formed and the grain size was smaller compared to the grain size of base metal with the average value of grain size are 63.6 µm and 18.3 µm for base metal and weld zone, respectively.

2.5 CONCLUSION

From this study, it was proved that the weld joint of AA7075 sheet metal can be produced using low power fiber laser. The following points were concluded from this experiment;

1. PW welding mode shows the significant result with keyhole penetration observed from the cross-section microstructure approximately 1 mm penetration depth compared to the CW mode. Weld joint can be produced due to half penetration depth was achieved.
2. Both welding mode shows same result of focused point. The focused point measured from the sample surface to the protective mirror was at F = 120 mm.
3. The microstructure changes from elongated grain in base metal into dendritic grain in weld zone. Defects such as underfill and porosity occurred because no shielding gas was used during experiment.

Low power fiber laser could be applied in welding high strength aluminium alloys such as AA 7075 which this method can participates successfully in automotive industry. This metal can be a replacement to conventional steel used such as for car body panel in automotive parts especially or applied for Taylor Welded Blanks (TWBs) application. For future recommendation, laser parameters such as shielding gas, incident of beam angles, and pulsed energy could be studied by using design of experiment (DOE) for a better weld result in welding AA 7075.

2.6 REFERENCE

[1] Shah LH, Akhtar Z, Ishak M. Investigation of Aluminum-Stainless Steel Dissimilar Weld Quality using Different Filler Metals. International Journal of Automotive and Mechanical Engineering 2013; 8: 1121-1131.

[2] Ghazali FA, Manurung YHP, Mohamed MA, Alias SK, Abdullah S. Effect of Process Parameters on the Mechanical Properties and Failure Behavior of Spot Welded Low Carbon Steel. Journal of Mechanical Engineering and Sciences, 2015; 8: 1489-1497.

[3] Ishak M, Islam MR, Sawa T. GMA Spot Welding of A7075-T651/AZ31B Dissimilar Alloys Using Stainless Steel Filler. Materials and Manufacturing Processes, 2014; 29(8): 980-987.

[4] Ishak M, Noordin NFM, Razali ASK, Shah LH, Romlay FRM. Effect of Filler on Weld Metal Structure of Aa6061 Aluminum Alloy by Tungsten Inert Gas Welding. International Journal of Automotive and Mechanical Engineering 2015; 11: 2438-2446.

[5] Assunção E, Quintino L, Miranda R. Comparative study of laser welding in tailor blanks for the automotive industry. The International Journal of Advanced Manufacturing Technology 2009; 49(1-4): 123-131.

[6] Tsuji M. IPG fibre lasers and aluminium welding applications. Welding International, 2009; 23(10): 717-722.

[7] Katayama S, Ogawa K. Laser weldability and ageing characteristics of welds: laser weldability of commercially available A7N01 alloy. Welding International, 2013; 27(3): 172-183.

[8] Kawahito Y, Matsumoto N, Abe Y, Katayama S. Laser absorption of aluminium alloy in high brightness and high power fibre laser welding. Welding International, 2012; 26(4): 275-281.

[9] Moon J, Katayama S, Mizutani M, Matsunawa A. Behaviour of laser induced plasma, keyhole and reflected light during laser welding with superimposed beams of different wavelengths. Welding International, 2003; 17(7): 524-533.

[10] Ishak M, Yamasaki K, Maekawa K. Lap Fillet Welding of Thin Sheet AZ31 Magnesium Alloy with Pulsed Nd:YAG Laser. Journal of Solid Mechanics and Materials Engineering, 2009; 3(9): 1045-1056.

[11] Katayama S, Nagayama H, Mizutani M, Kawahito Y. Fibre laser welding of aluminium alloy. Welding International, 2009; 23(10):744-752.

[12] Enz J, Riekehr S, Ventzke V, Sotirov N, Kashaev N. Laser Welding of High-strength Aluminium Alloys for the Sheet Metal Forming Process. In: Procedia CIRP, pp. 203-208, 2014.

[13] Wang JT, Zhang YK, Chen JF, Zhou JY, Ge MZ, Lu YL, Li XL. Effects of laser shock peening on stress corrosion behavior of 7075 aluminum alloy laser welded joints. Materials Science and Engineering: A, 2015; 647: 7-14.

[14] Fukuda T. Weldability of 7000 series aluminium alloy materials. Welding International, 2012 ;26(4): 256-269.

[15] Katayama S, Abe Y, Mizutani M, Kawahito Y. Deep Penetration Welding with High-Power Laser under Vacuum. Transactions of JWRI is published by Joining and Welding Research Institute, Osaka University, Ibaraki, Osaka 567-0047, Japan; 40(1), 2011.

[16] Jiang Z, Tao W, Yu K, Tan C, Chen Y, Li L, Li Z. Comparative study on fiber laser welding of GH3535 superalloy in continuous and pulsed waves. Materials & Design, 2016; 110: 728-739.

[17] Esraa FH, Hamed K, Fakhry M. Laser wavelength and energy effect on optical and structure properties for nano titanium oxide prepared by pulsed laser deposition. Iraqi Journal of Physics, 2014; 12(25): 62-68.

[18] Pang S, Chen X, Shao X, Gong S, Xiao J. Dynamics of vapor plume in transient keyhole during laser welding of stainless steel: Local evaporation, plume swing and gas entrapment into porosity. Optics and Lasers in Engineering, 2016; 82:28-40.

[19] Manoharan N, Sivashanmugam M, Ananthapadmanaban D, Ravi Kumar S. Investigation of microstructure and mechanical properties of GTAW and GMAW joints of AA7075 aluminium alloys. International Journal on Design and Manufacturing Technologies 2009; 2: 56-62.

[20] Chen S, Guillemot G, Gandin CA. Three-dimensional cellular automaton-finite element modeling of solidification grain structures for arc-welding processes. Acta Materialia, 2016; 115: 448-467.

[21] Dong HB. Analysis of Grain Selection during Directional Solidification of Gas Turbine Blades. In: World Congress on Engineering Vol II, London, United Kingdom; 2-4 July, 2007.

CHAPTER 3

TECHNICAL PAPER #2

Title:- Effect of shoulder to pin ratio on magnesium alloy friction stir welding

(IOP Conference Series: Materials Science and Engineering (2017) doi:10.1088/1757-899X/238/1/012008 – IOP-Scopus Indexed)

3.1 ABSTRACT

This study focuses on the effect of shoulder to pin diameter ratio on friction stir welding of magnesium alloy AZ31. Two pieces of AZ31 alloy with thickness of 2 mm were friction stir welded by using conventional milling machine. The shoulder to pin diameter ratio used in this experiment are 2.25, 2.5, 2.75, 3, 3.33, 3.66, 4.5, 5 and 5.5. The rotational speed and welding speed used in this study are 1000 rpm and 100 mm/min, respectively. Microstructure observation of welded area was studied by using optical microscope. Equiaxed grains were observed at the TMAZ and stir zone indicating fully plastic deformation. The grain size of stir zone increased with decreasing shoulder to pin ratio from ratio 3.33 to 5.5 due to higher heat input. It is observed that, surface galling and faying surface defect is produced when excessive heat input is applied. To evaluate the mechanical properties of this specimen, tensile test was used in this study. Shoulder to pin ratio 5.5 shows lowest tensile strength while shoulder to pin diameter ratio 3.33 shows highest tensile strength with weld efficiency 91 % from based metal.

3.2 INTRODUCTION

Weight reduction in automotive and aircraft industries is a main concern in improving fuel economy and reducing environmental pollutions [1].Recently, magnesium alloys are constantly gaining importance as lightweight structural materials for automotive applications [2]. The Mg alloys are especially attractive due to their low density, high specific stiffness and strength and also the recycling ability [3]. There have some problem in welding magnesium using

conventional fusion welding. Conventional fusion welding methods for joining magnesium alloys produce some defects such as porosity and hot crack, which deteriorate their mechanical properties due to the melting material [4]. Friction stir welding (FSW) is a welding method under solid state joining that involves no melting, i.e. welding below melting point and it can eliminate problem related to solidification.[5]. The advantages of FSW compared to other method are low distortion and shrinkage even in a long weld, excellent mechanical properties in fatigue, tensile and bend test, no arc or fume, can weld in all position, no filler wire needed, weight reduction because no usage of filler, can weld aluminum and copper more than 75 mm with only one pass and uses consumable tools, which means that the tool can used for many times [6].

In FSW, the non-consumable tool plays an important role in generating heat by means of friction to plasticize the materials to be welded**.** FSW tool have three different portions such shank, shoulder and pin. The pin diameter and shoulder diameter decide the quantum of heat generated during FSW [7]**.** The tool shoulder diameter is having directly proportional relationship with the heat generation due to friction [8], [9]. The pin of the tool generates the heat and stirs the material being welded but the shoulder also plays an important part by providing additional frictional treatment as well as preventing the plasticized material from escaping from the weld region [10].From the heating aspect, the relative size of pin and shoulder is important.

The heat generation is related to the mechanical and microstructure properties of welding that affect the quality of the welding. Vijayavel et al. (2014) investigated the effect of five different shoulder diameters to pin diameter (D/d) ratio on tensile properties and hardness of the friction stir processed welding of metal matrix composite [11]. Another researcher, Noor Zaman Khan et al. (2015) also investigate the effect of D/d ratio on joint quality but done at AA6063 [12]. Both researcher used fix shoulder diameter for the experiment. Some question appear would the result same if use vary shoulder and pin diameter for the ratio and applied at AZ31B magnesium alloy. It was found that not many studies regarding the ratio of tool shoulder diameter with pin diameter on tensile properties, macrostructure, microstructures and hardness of FSW joints of AZ31B with varying both shoulder and pin diameter. This study investigates the effect of shoulder to pin ratio on magnesium alloy AZ31 friction stir welding.

3.3 EXPERIMENTAL METHOD

Experiment was performed on plate of AZ31 magnesium alloy with 2 mm thickness. The dimensions of base metal plate were 50 mm (width) × 60 mm (length) and the plate was longitudinally butt welded using conventional milling machine. Table 3.1 shows the chemical compositions of AZ31 alloy that was checked using Foundry Mass Spectrometers machine. The

process parameters used for this experiment are given in Table 3.2 and the parameters are set from pre experiments, aiming at defect free specimens. The tilt angle was held constant at 3º based on several papers [13]–[16] and pre-tests. The welding tool material used is H13 steel with a taper cylindrical pin shape. The tool was processed by using a conventional lathe machine.

Table 3.1. Chemical compositions of AZ31 (wt.%).

Element	**Al**	**Zn**	**Mn**	**Si**	**Cu**	**Ca**	**Ni**	**Mg**
AZ31	2.87	0.99	0.239	0.0137	0.0183	0.0026	0.0015	Balance

Table 3.2 . Welding parameters and tool dimensions for FSW.

Process parameters	Values
Rotational speed(rpm)	1000
Welding speed (mm/min)	100
Pin length, l (mm)	1.8
Tool shoulder diameter, D (mm)	9, 10, 11
Pin diameter, d(mm)	2, 3, 4
Pin taper angle	10°
Tool ratio, D/d	2.5, 2.75, 3, 3.33, 3.66, 4.5, 5 and 5.5
Holder diameter, a(mm)	20
Holder length, b(mm)	20
Shoulder length, c(mm)	24

Mechanical characterizations were conducted using tensile test. The tensile test was prepared according to the ASTM-E8 standard. The tensile test was conducted with three repetitions and the average values were then presented in result and discussion. The data were recorded and analyzed accordingly. Cross-sectional samples were then cut and mounted to analyze their microstructures. The mounted sample was ground manually using 240, 320, 400 and 600-paper grid, successively. After the grinding process, the specimens were polished using 1, 3 and 6 µm DIAMAT Polycrystalline diamond to remove the major scratches and finally etched using 4.2 g picric acid, 10 ml acetic acid, 10 ml H2O and 70 ml ethanol. The microstructure of the weld specimens was observed using an optical microscope.

3.4 RESULTS AND DISCUSSION

3.4.1 Weld Appearance

Visual inspection was used to characterize the weld bead defect and appearance. From figure below, observed that Fig. 3.1 (i)-(m) shows smooth weld appearance while (a) ,(b) and (g) shows small flash at retreating side. Specimen with pin ratio 4.5, 5, and 5.5 shows flash defect. Most experiments that have flashed come from large tool ratio with small pin area that is 2 mm pin diameter. This is due to the higher heat generation at the weld center. This statement also

support by Saravan et al. 2016 that shoulder give more friction resulting in higher heat generation while small pin diameter affect the splitting microstructure into fine grain size [17]. Experiment no 2 shows surface galling defect due to the sticking material at the pin [18] and ribbon flash is due to the over dwell time. When a longer time is taken after the initial plunge of the tool pin, it induces more heat to the specimen and increases the fluidity. The extra fluid (metal) will split out of the weld area, causing this defect [19]. All the defect will degrade the mechanical properties [18].

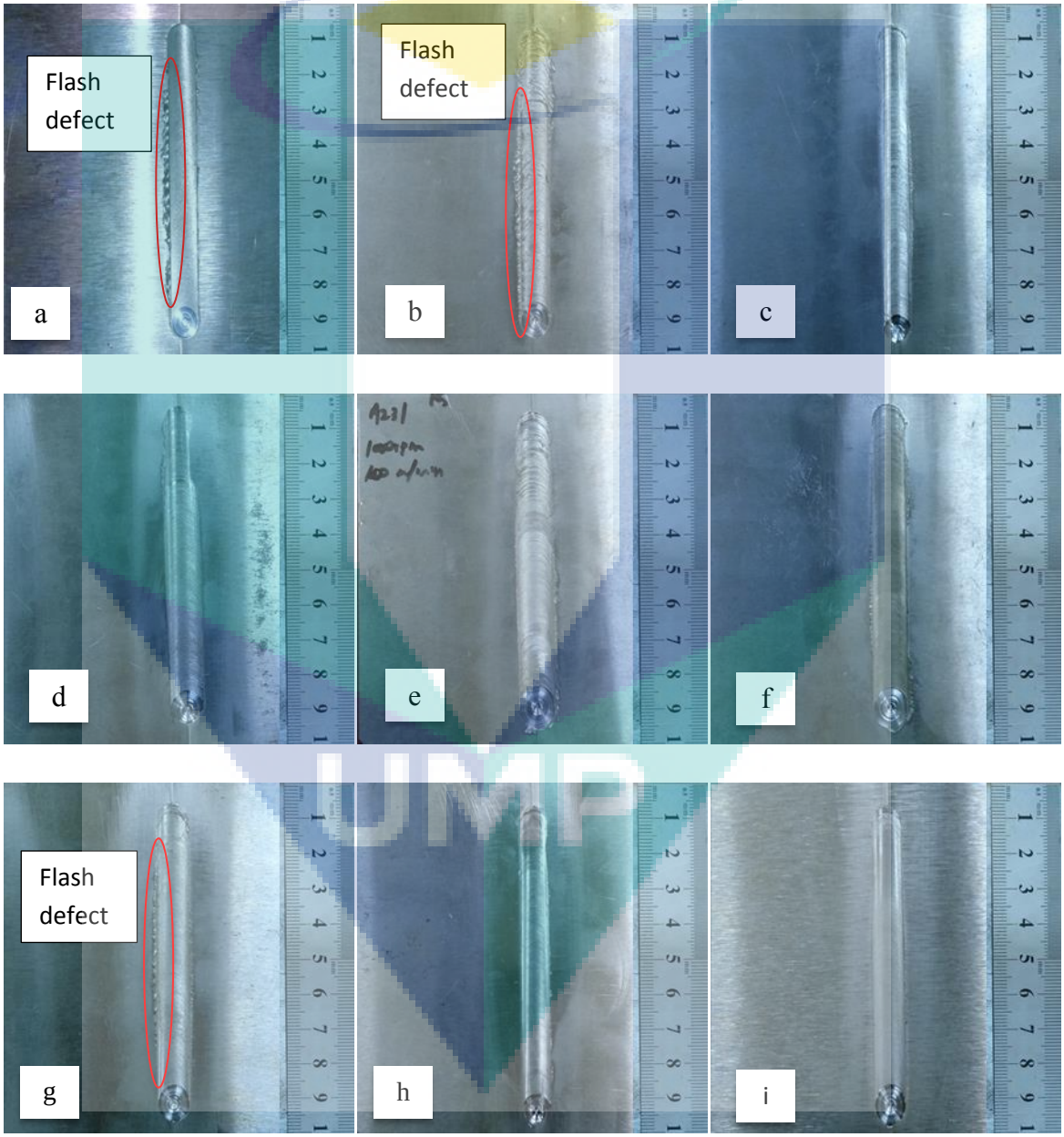

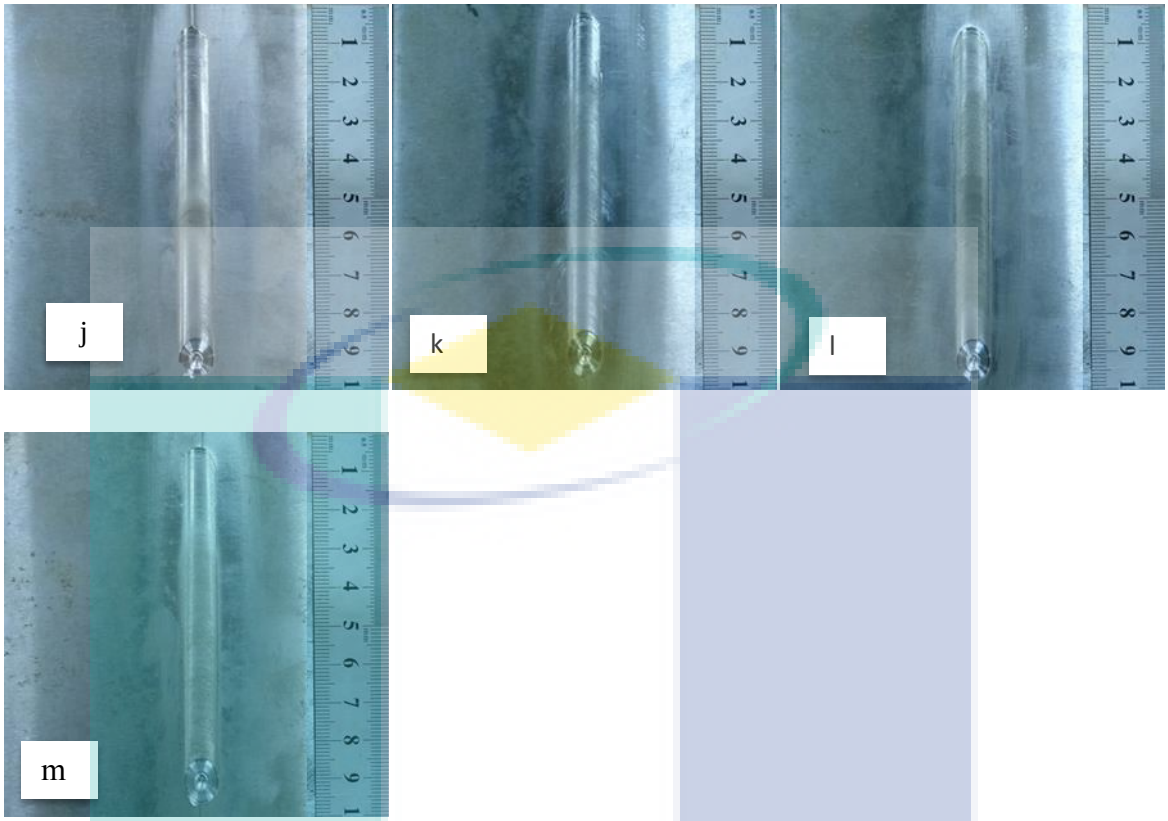

Fig. 3.1. Weld appearances for shoulder to pin diameter ratio D/d on friction stir welding. a) ratio 4.5 , b) ratio 5.5 ,c) ratio 2.25, d) ratio 2.75 ,e) ratio 3 ,f) ratio 3.66 ,g) ratio 5, h) ratio 2.5 , i) ratio 3.33 ,j) ratio 3.33 , k) ratio 3.33 ,l) ratio 3.33 ,m) ratio 3.33

3.4.2 Tensile properties of welded joints

The tensile test was conducted and the ultimate tensile strength (UTS) data shown in Table 3. The median from three samples for each specimen was taken to avoid the outliers from the overall samples.

Table 3.3. Ultimate tensile strength for shoulder to pin ratio friction stir welding.

Exp. No.	Shoulder Diameter	Pin Diameter	Tool Ratio	Ultimate tensile strength (MPa)
1	9	2	4.50	164.236
2	10	2	5.5	158.105
3	9	4	2.25	194.275
4	11	4	2.75	192.078
5	9	3	3	221.674
6	11	3	3.66	219.399
7	10	2	5	179.350

8	10	4	2.5	212.413
9	10	3	3.33	241.391
10	10	3	3.33	236.019
11	10	3	3.33	241.149
12	10	3	3.33	239.630
13	10	3	3.33	237.347

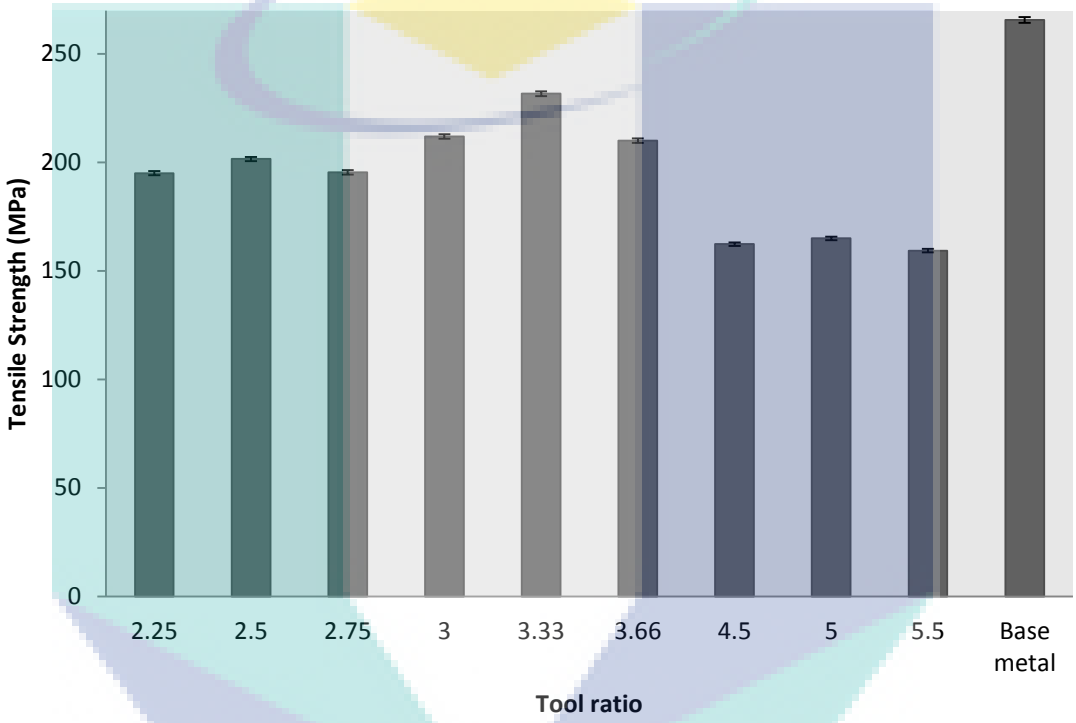

Fig. 3. 2. Ultimate tensile strength of different pin ratio

According to the table, specimen 2 and 9 show the lowest and the highest UTS, respectively. The shoulder to pin ratio (D/d) 5.5 with shoulder diameter 11 and pin diameter 2 resulted in the lowest UTS value of 158.105 MPa. The shoulder to pin ratio (D/d) 3.3 with shoulder diameter 10 and pin diameter 3 resulted in the highest UTS value of 241.391 MPa. This value is near to the base metal UTS which is 265.6 MPa with 91 % weld efficiency. Fig. 3. 2 shows the UTS of the welding joint and the base metals. The tensile strength trend shows that the strength are increase with increasing the tool ratio until tool ratio 3.33 and it decrease with increasing tool ratio after tool ratio 3.33. Tool ratio 4.5, 5 and 5.5 shows low tensile strength due to the flash defect shows in Fig. 3.1. Flash may occur due to the improper parameter setting [20] that cause thinning the weld and result in decreasing the mechanical properties [18].

3.4.3 Metallurgical analysis

The weldability of magnesium alloy by using fiction stir welding was achieved through the excellent mechanical properties. Besides the mechanical properties, macro and microstructure of the welded area are also an important characteristic in identifying the ability of the material to form a good weld.The sample for macrostructure observation was taken based on the tensile strength results; the lowest UTS and the highest UTS. The microstructural image was taken by using an optical microscope with ×50 magnifications. The cross sections of the welded area for lowest and highest tensile sample are shown in

Fig. 3.4 and Fig. 3.6, respectively. It was observed that all specimens show the complete penetration. However, there were several defects that can be identified through the cross section of the completed penetration specimen such as surface galling of weld surface and faying surface defect, as well as the porosity existent in the welded area as shown in

Fig. 3.4. Excessive hot weld is one of the factors existing surface galling and faying surface defect. Thus, the proper combination shoulder to pin diameter ratio are important to make sure the heat generation are sufficient for the welding.

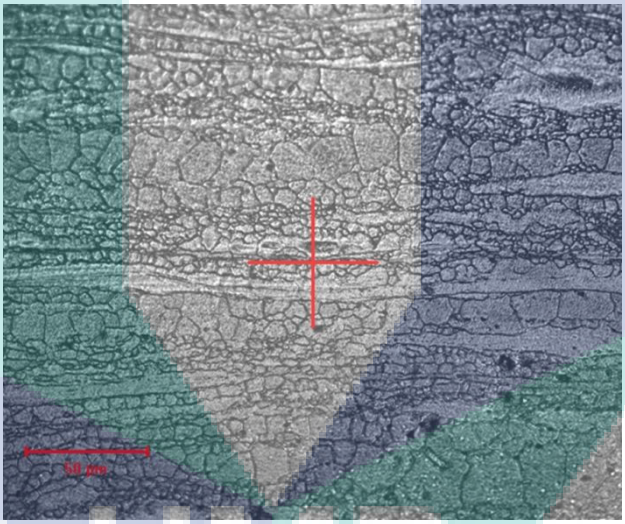

Fig. 3.3. Microstructure of based metal (BM) AZ31 Magnesium alloy

The major FSW regions can be observed, namely the base metal (BM), heat affected zone (HAZ), thermo mechanically affected zone (TMAZ) and weld zone (WZ). Fig. 3.3 shows typical microstructure of base metal (BM) before friction stir weld. The base metal exhibit coarse microstructure with elongated and pancake grain size. Fig. 3.5 (b) and (c) shows the TMAZ and SZ for the lowest tensile strength. The grain size at SZ shows fine grain size. TMAZ shows elongated grain compare to SZ with average grain size 10.32 µm for TMAZ and 6.61 µm for SZ. HAZ shows uneven grain boundary with average grain size 15.944 µm.

Shoulder give more friction resulting in higher heat generation but the small pin diameter affect the splitting microstructure into fine grain size [17]. Fig. 3.6 shows cross sectional microstructure for ratio 3.33 with highest tensile strength. SZ and TMAZ at ratio 3.33

consist of fine and equiaxed grains which show that recrystallization already occur. Small grain size affect the tensile strength due to the homogeneous in whole area and crystal orientations of such grains are rather randomly distributed [21]. TMAZ shows elongated grain compare to SZ with average grain size 6.497 µm and 2.907 µm respectively. HAZ shows coarser and elongated grain size compare to SZ and TMAZ but small HAZ grain size compare to tool ratio 5.5. The stir zone exhibit fine grain compared to base metal which is coarse grain.

This behavior is due to dynamic recrystallization from the simultaneous deformation and heat input during welding process where the heat generated from the interaction of the pin tool deformed the grain boundaries [22] lead to the higher tensile strength of specimen. Grain structures for TMAZ in Fig. 3.7 have slightly changed in grain structure due to the heat input that is sufficiently heated to undergo deformation from its original grain boundaries. TMAZ region undergo plastic deformation but recrystallization did not take place in this region due to inadequate deformation strain [23]. In HAZ, the magnesium alloy experienced thermal cycle but only little plastic deformation occurred. The increase in grain size consequently decreased the tensile strength [24]. Smaller grain size will affect the tensile strength due to the dislocation movement in the material. By reducing the dislocation movement of grain (fine grain size) ,the mechanical strength of material can be improve due to the metal plastically hard to deform [25].

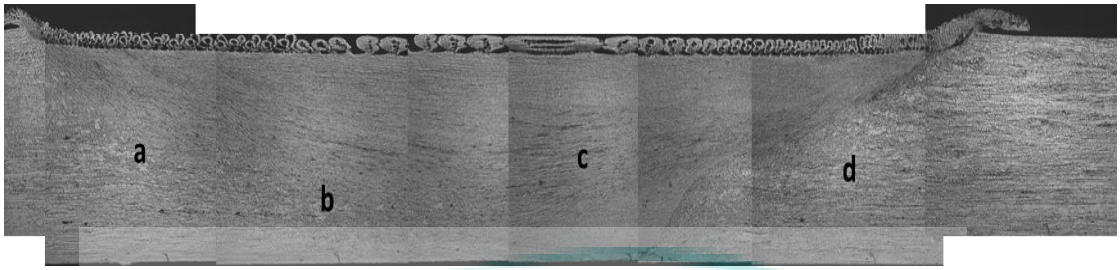

Fig. 3.4. Cross sectional macrostructure for ratio 5.5 with lowest Ultimate Tensile Strength. A) location retreating side HAZ, b) location TMAZ, c) location SZ, (d) location advancing side HAZ

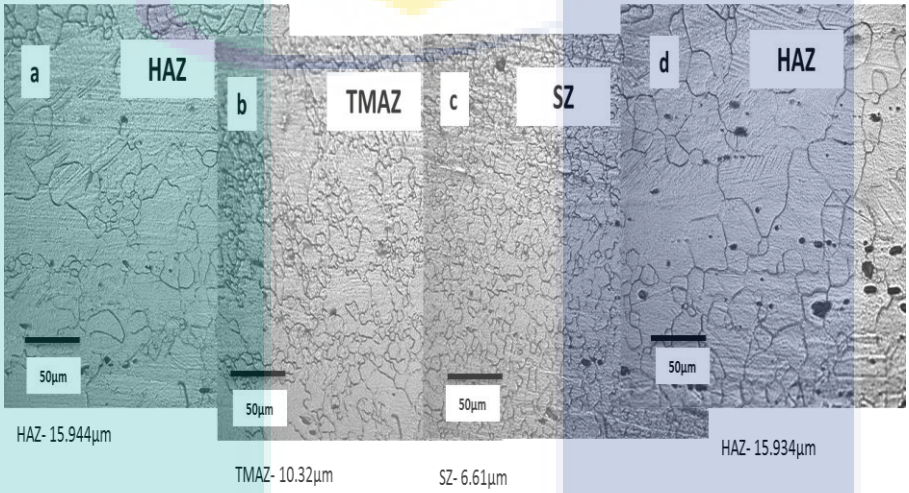

Fig. 3.5. Microstructure of ratio 5.5 (a) Retreating side HAZ (b) TMAZ (c) SZ and (d) Advancing side HAZ

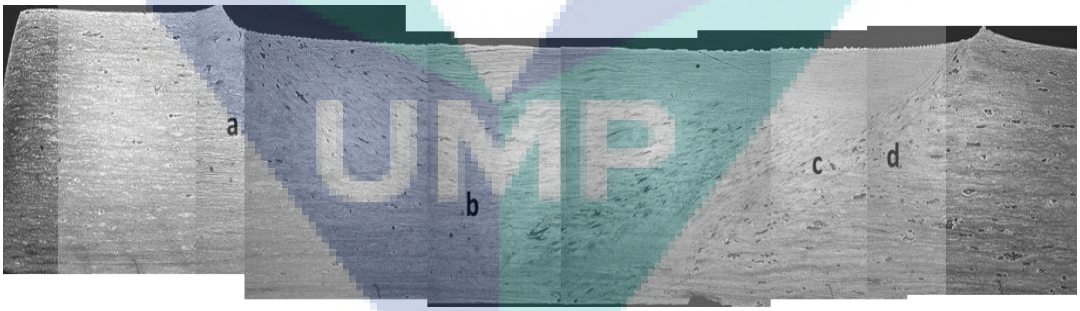

Fig. 3.6. Cross sectional macrostructure for ratio 3.33 with highest Ultimate Tensile Strength a) location retreating side HAZ, b) location SZ ,c) location TMAZ, d) location advancing side HAZ

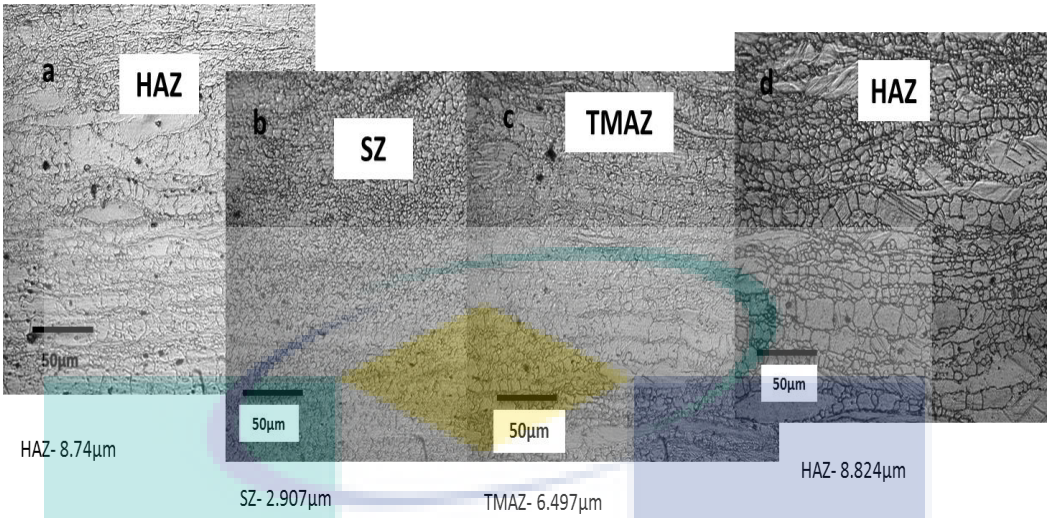

Fig. 3.7. Microstructure of ratio 3.33 (a) Retreating side HAZ (b) TMAZ (c) SZ and (d) Advancing side HAZ

3.5 CONCLUSION

1. Thickness of 2 mm magnesium alloy AZ31 plates were successfully welded by using friction stir welding process with shoulder to pin diameter ratio 2.5, 2.75, 3, 3.33, 3.66, 4.5, 5 and 5.5 with 1000 rpm rotational speed and 100 mm/min welding speed
2. All specimen produce sound quality joints with minimal defects. The best weld appearance can be observed in small ratio from 2.25 till ratio 3.33. Ratio 3.66 until 5.5 shows some defect such as little flash defect. Fine grain size can be seen in WZ and TMAZ and coarser grain size can be seen in the HAZ. The average grain size for D/d ratio 3.33 shows smaller grain size compare to other tool ratio. Smaller grain size will affect the tensile strength of the specimens. The D/d tool ratio 3.33 yielded the highest tensile value of 241.391 MPa due to the fine grain size and good weld appearance. Therefore the optimum D/d shoulder to pin ratio for magnesium alloy AZ31 are at ratio 3.33 gives better weld appearance and high tensile strength.

3.6 REFERENCE

[1] X. Cao and M. Jahazi, "Effect of welding speed on the quality of friction stir welded butt joints of a magnesium alloy," *Mater. Des.*, vol. 30, no. 6, pp. 2033–2042, 2009.

[2] G. Sahu, "A Brief Review on MG Alloys Their Properties and Application," *Int. J. Adv. Res. Sci. Eng.*, vol. 8354, no. 4, pp. 65–71, 2015.

[3] C. Blawert, N. Hort, and K. U. Kainer, "Automotive Applications of Magnesium and Its Alloys," *Magnesium*, vol. 57, no. 4, pp. 397–408, 2006.

[4] S. Rajakumar, a. Razalrose, and V. Balasubramanian, "Friction stir welding of AZ61A magnesium alloy: A parametric study," *Int. J. Adv. Manuf. Technol.*, vol. 68, no. 1–4, pp. 277–292, 2013.

[5] R. S. Mishra and Z. Y. Ma, "Friction stir welding and processing," *Mater. Sci. Eng. R Reports*, vol. 50, no. 1–2, pp. 1–78, Aug. 2005.

[6] W. M. U. Thomas, E. D. Nicholas, A. Hall, and C. Cb, "Friction stir welding for the transportation industries," vol. 18, pp. 269–273, 1998.

[7] S. Malarvizhi and V. Balasubramanian, “Influences of tool shoulder diameter to plate thickness ratio (D/T) on stir zone formation and tensile properties of friction stir welded dissimilar joints of AA6061 aluminum–AZ31B magnesium alloys,” *Mater. Des.*, vol. 40, pp. 453–460, Sep. 2012.

[8] G. M. Reddy, P. Mastanaiah, C. V. S. Murthy, and T. Mohandas, “Microstructure , Residual Stress Distribution and Mechanical Properties of Friction-Stir AA 6061 Aluminium Alloy Weldments,” 2006.

[9] A. A. N. A. Oosterkamp, L. Djapic Oosterkamp, “‘ Kissing Bond ’ Phenomena in Solid-State Welds of Aluminum Alloys,” no. August, pp. 225–231, 2004.

[10] S. Rajakumar, C. Muralidharan, and V. Balasubramanian, “Influence of friction stir welding process and tool parameters on strength properties of AA7075-T6 aluminium alloy joints,” *Mater. Des.*, vol. 32, no. 2, pp. 535–549, Feb. 2011.

[11] P. Vijayavel, V. Balasubramanian, and S. Sundaram, “Effect of shoulder diameter to pin diameter (D/d) ratio on tensile strength and ductility of friction stir processed LM25AA-5% SiCp metal matrix composites,” *Mater. Des.*, vol. 57, pp. 1–9, 2014.

[12] N. Z. Khan, Z. a. Khan, and A. N. Siddiquee, “Effect of Shoulder Diameter to Pin Diameter (D/d) Ratio on Tensile Strength of Friction Stir Welded 6063 Aluminium Alloy,” *Mater. Today Proc.*, vol. 2, no. 4–5, pp. 1450–1457, 2015.

[13] Y. C. Chen and K. Nakata, “Friction stir lap joining aluminum and magnesium alloys,” *Scr. Mater.*, vol. 58, no. 6, pp. 433–436, Mar. 2008.

[14] A. A. M. da Silva, E. Arruti, G. Janeiro, E. Aldanondo, P. Alvarez, and A. Echeverria, “Material flow and mechanical behaviour of dissimilar AA2024-T3 and AA7075-T6 aluminium alloys friction stir welds,” *Mater. Des.*, vol. 32, no. 4, pp. 2021–2027, Apr. 2011.

[15] N. H. Othman, L. H. Shah, and M. Ishak, “Mechanical and microstructural characterization of single and double pass Aluminum AA6061 friction stir weld joints,” *IOP Conf. Ser. Mater. Sci. Eng.*, vol. 100, p. 012016, 2015.

[16] N. a. a. Sathari, a. R. Razali, M. Ishak, and L. H. Shah, “Mechanical Strength of Dissimilar Aa7075 and Aa6061 Aluminum Alloys Using Friction Stir Welding,” *Int. J. Automot. Mech. Eng.*, vol. 11, no. JUNE, pp. 2713–2721, 2015.

[17] V. Saravanan, S. Rajakumar, N. Banerjee, and R. Amuthakkannan, “Effect of shoulder diameter to pin diameter ratio on microstructure and mechanical properties of dissimilar friction stir welded AA2024-T6 and AA7075-T6 aluminum alloy joints,” *Int. J. Adv. Manuf. Technol.*, 2016.

[18] W. J. Arbegast, “Friction Stir Joining : Characteristic Defects,” *Adv. Mater. Process. Cent. MET*, vol. 6, no. October, pp. 1–30, 2003.

[19] A. S. Babu and C. Devanathan, “An Overview of Friction Stir Welding,” *Int. J. Res. Mech. Eng. Technol.*, vol. 3, no. 2, pp. 259–265, 2013.

[20] B. T. Gibson, D. H. Lammlein, T. J. Prater, W. R. Longhurst, C. D. Cox, M. C. Ballun, K. J. Dharmaraj, G. E. Cook, and A. M. Strauss, “Friction stir welding: Process, automation, and control,” *J. Manuf. Process.*, vol. 16, no. 1, pp. 1–18, Jun. 2014.

[21] A. Goloborodko, T. Ito, X. Yun, Y. Motohashi, and G. Itoh, “Friction Stir Welding of a Commercial 7075-T6 Aluminum Alloy: Grain Refinement, Thermal Stability and Tensile Properties,” *Mater. Trans.*, vol. 45, no. 8, pp. 2503–2508, 2004.

[22] H. I. Dawood, K. S. Mohammed, and M. Y. Rajab, “Advantages of the Green Solid State FSW over the Conventional GMAW Process,” *Adv. Mater. Sci. Eng.*, vol. 2014, pp. 1–10, 2014.

[23] D. Lohwasser and Z. Chen, *Friction stir welding: From basics to applications*. Cambridge, England: Woodhead Publishing Limited, 2010.

[24] S. Rajakumar, C. Muralidharan, and V. Balasubramanian, “Establishing empirical relationships to predict grain size and tensile strength of friction stir welded AA 6061-T6 aluminium alloy joints,” *Trans. Nonferrous Met. Soc. China*, vol. 20, no. 10, pp. 1863–1872, 2010.

[25] R. Abbaschian, L. Abbaschian, and R. E. Reed-Hill, *Physical Metallurgy Principles*. Cengage, 2009.

UMP

CHAPTER 4

TECHNICAL PAPER #3

Title:- Dissimilar welding of A7075-T651 and AZ31B alloys by gas metal arc plug welding method.

(International Journal of Advance Manufacturing Technology (2017)
doi:10.1007/s00170-016-8993-6 – ISI Indexed)

4.1 ABSTRACT

Innovative welding techniques allow for the fabrication of light, high-specific-strength, and fuelsaving Al and Mg alloys for use in transportation industries. Furthermore, these techniques have minimal detrimental impact on the environment. However, the poor mechanical properties of joints resulting from the formation of brittle AlmMgn intermetallic compounds are key barriers to joining Al and Mg alloys. To date, a proper solution to this problem has not yet been provided. The aim of this research was to investigate the mechanical and metallurgical properties of the joint between AZ31B and A7075-T651 alloys welded by a new technique called gas metal arc plug welding method. ER5356 aluminum wire was used as a filler. The yield and ultimate tensile strengths as well as impact toughness of the joints were measured. The fracture surface was investigated by scanning electron microscopy and energy-dispersive X-ray spectroscopy. The maximum ultimate tensile strength and impact toughness of the joints were 89 and 84 % of those of the AZ31B parent alloy, respectively. Generally, the joints failed in the ER5356 nugget, whereas some failed in the AZ31B alloy. No fracture was observed in the A7075-T65 alloy. Brittle fracture mechanism was observed for all the joints. In conclusion, the proposed welding technique can allow for better mechanical properties of joints for dissimilar welding of aluminium and magnesium alloys.

4.2 INTRODUCTION

Lightweight structures are of primary importance in the automotive, aviation, aerospace, and marine industries because they can reduce fuel consumption and greenhouse gas emissions [1]. Although steel is the principal material used in transportation industries, such materials as Al and Mg have drawn considerable attention because of their

lightweight and fuelsaving properties [2]. Accordingly, researchers have searched for high-strength and fuel-efficient (i.e., lightweight) metals [3]. At present, Al and Mg are classified as the lightest and most important nonferrous metals, as well as the most promising materials in manufacturing industries [4]. Alloys from both metals have been continuously and extensively researched during the past decades because of their practical industrial applications. In fact, various Al and Mg alloys are anticipated to become the fundamental materials in almost all structures in the near future. In most land, water, and air transportation systems, particularly in the automotive industry, both Al and Mg alloys are used in the structures of the aforementioned systems. Thus, a successful welding technique is of utmost importance to combine these two alloys [5]. The main difficulties in welding these two alloys result from the differences in their physical and chemical properties. Moreover, Al–Mg reaction causes the formation of very brittle and fragile AlmMg n-type intermetallic compounds (IMCs). Consequently, the joint formed with these two alloys possesses very low strength, and it can be easily fractured, even by hand. An appropriate welding technique that can reduce or avoid the formation of AlmMgn IMCs in the welding joint should be introduced to achieve a joint with good mechanical and metallurgical properties [5]. Both Al and Mg alloys possess numerous attractive physical, mechanical, and chemical properties, such as light weight, excellent thermal conductivity and electrical conductivity, high specific strength, high stiffness, good formability, high durability, recyclability, excellent corrosion resistance, low-cost maintenance, and high recovery potential [3, 4]. With the requirements for fuel economy and environmental conservation, specific strength is and will continue to be a key factor in material selection [5]. Recently, numerous industries have shown considerable interest to Al and Mg alloys for their potential usability in an extensive array of applications. To enhance the properties of these alloys and develop innovative and reliable welding technologies, several scholars [6] have investigated the use of these two alloys in compound structures to reduce vehicle weight and cost and achieve better mechanical properties, particularly in key engineering applications, such as automotive [7], marine [8], aviation, aerospace [9], and electronics [2, 8, 10, 11]. Given the extensive use of these alloys as structural materials, innovative ways to join them are essential [5, 12–16]. Joining these two alloys may allow for enhanced design flexibility and quality of components through compound structures [17]. Furthermore, joining by

welding of Mg and Al alloys can improve the flexibility and availability of several components substantially [7].

Accordingly, the effectiveness of the joint between Al and Mg alloys should be investigated. In addition, problems in Al and Mg welding must be addressed and solved [12, 16]. The application of modern industrial materials has also made the welding technology for Al and Mg alloys important [17]. Welding joints significantly affect the life span, safety, endurance, and quality of structures [2]. They are also highly considered in a wide range of applications of advanced materials, such as Al and Mg alloys. At present, gas metal arc (GMA), friction stir welding (FSW), tungsten inert gas (TIG), laser, hybrid laser/TIG, neodymium-doped yttrium– aluminum garnet, explosive, resistance spot welding (RSW), cold metal transfer, and electron beam welding methods have been utilized for joining both alloys [10, 18–20]. Few unconventional approaches, including vacuum diffusion bonding and hybrid FSW, have been tried to enhance the mechanical properties of welding joints. However, most of the attempts achieved either partially satisfactory or unsatisfactory results because Al2Mg3-, Mg2Al13-, and Mg17Al12-type IMCs are formed at the Al–Mg interface. These IMCs are incredibly brittle and degrade the mechanical properties of the joints [15, 21, 22].

Certain welding configurations and the selection of appropriate parameters within appropriate ranges could be among the solutions to reduce or inhibit the formation of AlmMgn IMCs. The maximum strength of the welding joint between Al and Mg alloys achieved thus far is only 67 % of the maximum strength of the Al-based alloy, which is very low [16]. Therefore, extensive research should be undertaken to establish reliable welding techniques between Al and Mg alloys. To address the aforementioned problems and enhance the traditional GMA welding technique [10, 23, 24], the current study presented a new GMA plug welding method using ER5356 Al filler to join A7075-T651 and AZ31B alloys. GMA plug welding is similar to welding in single-point through holes without moving the workpiece or welding gun. In this joining method, the lower and upper pieces are in a lap configuration.

A lap joint is one of the most common joint shapes in the automotive and aviation industries, and it is normally achieved using the RSW method. However, using RSW to weld any Al alloy to any Mg alloy causes the formation of AlmMgn-type IMCs, which deteriorate the essential mechanical properties of the joint [25]. By contrast, the proposed technique can minimize the formation of AlmMgn IMCs by reducing the

direct bonding area between the Al and Mg alloys to improve the mechanical properties of the joint, such as yield strength (YS), ultimate tensile strength (UTS), and fracture toughness. GMA plug welding method can also expedite the combination and extensive use of Al and Mg alloys in the mass production of lightweight vehicle structures in the marine, automotive, aviation, and aerospace industries. Therefore, in this study, the UTS and impact toughness of the joint between A7075-T651 Al and AZ31B Mg alloys were examined. Metallurgical investigations of the fracture surface and welding cross sections were also conducted by optical microscopy, scanning electron microscopy (SEM), and energy-dispersive X-ray spectroscopy (EDX).

4.3 RESEARCH METHODOLOGY

4.3.1 Experimental Method

From A7075-T651 and AZ31B alloy sheets, 75× 70× 2 mm (length× width × depth) plates were cut by a shear-cutting machine. Then, 3.5-mm-diameter holes were drilled in each Al and Mg plate, as shown in Fig. 4.1. The alloy plates were rubbed on flat mechanical files to refine and polish the edges. Each plate was then polished using 360-grit emery paper to remove the oxide films on the faying surfaces. Before welding, the pieces were wiped with an acetone solution to remove impurities, such as oil and grease, which are typically present after cutting and drilling processes. The AZ31B alloy plate was placed on top of the A7075-T651 alloy plate, overlapping by 20 mm. The shielding gasses used were 98 % Ar+ 2 % O2 throughout the welding process. First, the GMA plug welding was applied to the through holes on the A7075-T651 side. Subsequently, the A7075-T651 side was positioned facing downward to weld the AZ31B alloy side. The welding time was 5 s for the A7075-T651 alloy side and 3 s for the AZ31B alloy side. The chemical compositions of the parent alloys and the filler material are shown in Table 4.1.

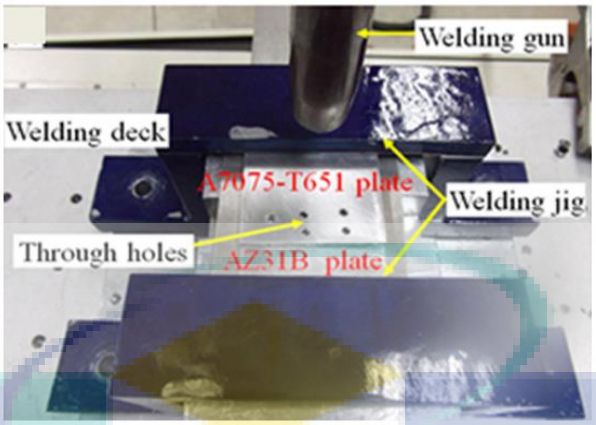

Fig. 4.1. Illustration of the welding layout

Table 4.1. Chemical compositions of A7075-T651, AZ31B alloys and ER5356 Al fillers (wt %) [24–30]

Element	A7075-T651	AZ31B	ER5356
Al	Balance	2.5-3.5	Balance
C	-	-	-
Ca	-	0.04	-
Co	-	-	-
Cr	0.23	-	0.06
Cu	1.6-1.8	-	0.011
Fe	0.5	-	0.2
Mg	2.5-2.7	Balance	4.6-5.0
Mn	0.3	<1.0	0.15
Mo	-	-	-
Ni	-	-	-
Si	0.4	<0.2	0.2
Ti	0.2	-	>0.05
Zn	5.6	0.5-2.0	>0.1

The design of experiments (DOE) was completed by the Box–Behnken technique of the response surface method. The DOE and the welding powers are shown in Table 4.2. Twentysix sets of experimentations were completed in replicate based on the DOE. From the welded workpieces, tensile and toughness specimens were prepared by EDM wire cutting machine according to standard dimensions. Tensile test specimens complied with the ASTM E8M-04 standard (length 100 mm; grip length 20 mm; grip width 20 mm; gauge length 40 mm; width of reduced section 12.5 mm; fillet radius of reduced section 12.5 mm) [26].

Table 4.2. Design of experiments and welding power

Exp. No	GSR (L/min)	TWD (mm)	WV (V)	WC (A)	Welding Power (V x C), W	Yield strength (MPa)	UTS (MPa)	Impact Energy, CVN, (J)
1	5	8	15	90	1350	204.14	5.33	19.11

2	25	8	15	90	1350	112.65	3.92	13.69
3	5	12	15	90	1350	112.15	3.93	14.11
4	25	12	15	90	1350	177.78	5.41	18.91
5	15	10	10	65	650	61.19	3.18	10.01
6	15	10	20	65	1300	101.68	2.54	9.550
7	15	10	10	115	1150	155.00	4.29	15.50
8	15	10	20	115	2300	70.770	1.95	7.173
9	5	10	15	65	975	104.69	3.65	12.67
10	25	10	15	65	975	147.82	4.93	17.38
11	5	10	15	115	1725	193.00	4.92	19.07
12	25	10	15	115	1725	117.38	4.27	13.92
13	15	8	10	90	900	111.89	3.26	11.37
14	15	12	10	90	900	128.74	4.81	16.02
15	15	8	20	90	1800	122.10	3.15	11.03
16	15	12	20	90	1800	73.630	1.86	7.321
17	15	10	15	90	1350	109.57	3.89	14.09
18	5	10	10	90	900	106.57	3.68	13.14
19	25	10	10	90	900	84.780	3.16	10.34
20	5	10	20	90	1800	81.170	1.83	6.499
21	25	10	20	90	1800	70.770	2.22	8.693
22	15	8	15	65	975	121.36	4.08	14.11
23	15	12	15	65	975	178.24	5.66	18.72
24	15	8	15	115	1725	226.28	7.42	20.22
25	15	12	15	115	1725	136.11	4.77	16.27
26	15	10	15	90	1350	112.35	4.97	14.40
A7075	464.87	590.05	8.82	35.15	464.87	590.05	8.82	35.15
AZ31B	203.63	254.05	8.67	28.03	203.63	254.05	8.67	28.03

The specimens were tested in an INSTRON universal testing machine at room temperature and a strain rate of 2 mm/min with 50 kN load to determine the YS and UTS of the welding joints. Impact toughness specimens were prepared according to the ASTM D5045 standard (length 55 mm; width 10 mm; U-notch depth 2 mm; U-notch width 0.5 mm; notch root radius 0.25 mm) and tested in a Zwick Roell digital impact tester to determine the absorbed impact energy (CVN) of the joint [27]. The test was performed with a 15-J capacity and 390-mm-long pendulum.

The angle of release was 160°, and room temperature means 30 °C [28]. Welding an Al alloy to a Mg alloy is an entirely new method and has not been documented. In this new method, an ER5356 Al filler was used because of its moderate strength and toughness and compatibility with both A7075-T651 and AZ31B alloys. The ER5356 Al filler were formed into nuggets in the through holes to affix the two alloys strongly. Thus, the two dissimilar alloys were joined through the ER5356 Al nuggets and the direct bonding area. Through this method, the formation of AlmMgn-type IMCs was minimized during the welding of these two alloys. Consequently, failure would most probably occur on the weakest AZ31B alloy side or the relatively weak

ER5356 Al nugget side. In this study, the maximum attainable joint fracture toughness was targeted.

4.4 RESULTS AND DISCUSSION

4.4.1 Comparison of the strength and impact toughness of the joints

YS, UTS, and absorbed impact energy (CVN) values are tabulated in Table 4.2. As shown in Table 4.2, the joint fabricated at a gas-flow rate (GSR) of 15 L/min, tip-to-work distance (TWD) of 10 mm, welding voltage (WV) of 20 V, and welding current (WC) of 115 A achieved the lowest YS (57.28 MPa).

By contrast, the joint fabricated at a GSR of 5 L/min, TWD of 10 mm, WV of 15 V, and WC of 115 A achieved the highest YS (176.30 MPa). The joint fabricated at a GSR of 15 L/min, TWD of 10 mm, WV of 10 V, and WC of 65 A achieved the lowest UTS (61.19 MPa). By contrast, the joint fabricated at a GSR of 15 L/min, TWD of 8 mm, WVof 15 V, and WC of 115 A achieved the highest UTS (226.28 MPa, which is 89.07 % of the UTS of the AZ31B parent alloy). The joint fabricated at a GSR of 5 L/min, TWD of 10 mm, WVof 20 V, and WC of 90 A achieved the lowest impact toughness as indicated by CVN (1.8 J). On the contrary, the joint fabricated at a GSR of 15 L/min, TWD of 8 mm, WV of 15 V, and WC of 115 A achieved the highest impact toughness (7.42 J, which is 85.5 % of the impact toughness of the AZ31B parent alloy). Thus, the recommended welding parameters for the novel welding method are 15 L/min GSR, 8 mm TWD, 15 V WV, and 115 AWC as they allow for high tensile strength and good impact toughness.

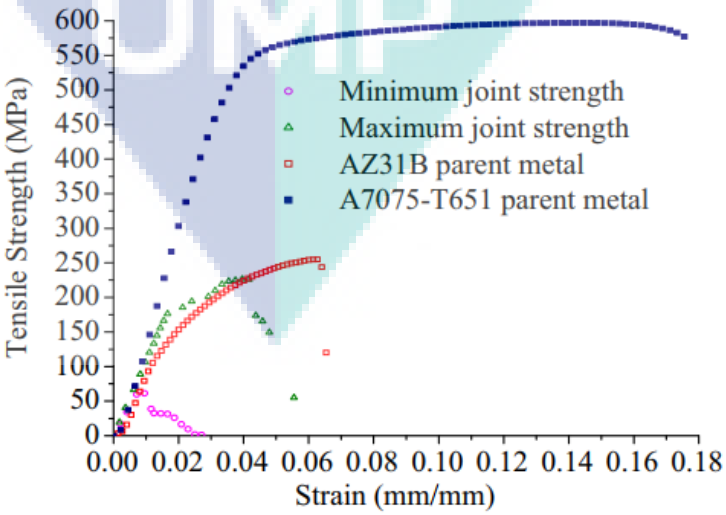

Fig. 4.2. Comparison of stress strain curves for joints with minimum and maximum UTS and parent metals

Consequently, better and significantly improved mechanical properties were achieved with the use of an Al filler. Most of the welding joints failed in the Al nugget. The strengths of AZ31B (σs, 220–290 MPa) or A7075-T651 (σs, 570 MPa) parent alloys were each higher than that of the filler was considered the strength of the joints. The joints achieved better mechanical properties mainly because these joints were fabricated at a medium welding power (1725 W), which resulted in the proper melting, bonding, and formation of fine grains and precipitates. Less pores, voids, and cracks also formed at a medium welding power. By contrast, a low welding power resulted in a lack of fusion and improper bonding, whereas a high welding power caused coarse grains in the fusion zone and the formation of voids, pores, cracks, oxides, and burn-throughs [29]. Fig. 4.2 illustrates the mechanical properties of the welding joints through the stress–strain curves generated by tensile testing and compares the curves with those of the parent alloys. In this study, only the stress–strain curves for the minimum and maximum UTSs were considered. From the stress–strain curves, the YS and UTS of any joint can be derived. As shown in Fig. 4.2, the curves of the joints with minimum and maximum UTSs both exhibited lower elongation and lower stress level than those of their AZ31B and A7075-T651 parent alloys before reaching UTS. This result proved that both joints exhibited lower plasticity but the joint with the maximum UTS had higher elongation and higher plasticity than the joint with the minimum UTS. This result also proved that the Al filler had lower ductility [30].

4.4.2 Macrostructural and microstructural analysis

Fig. 4.3 shows the macrostructural view of the cross sections of the welding joints. The macro cross sections of the welding joints consisted of three parts: AZ31B alloy, A7075-T651 alloy, and ER5356 Al nugget. Although most nuggets were fully constructed, filling the spaces in the through holes of the A7075-T651 and AZ31B parent alloys, some nuggets were not. This condition might be due to the difference in the viscosity levels of the molten Al fillers at different welding powers. At a low welding power, the molten fillers exhibited increased viscosity and decreased fluidity because of the low welding heat. Consequently, they showed reluctance in spreading to fill the through holes. By contrast, at a high welding power, the molten fillers exhibited

decreased viscosity and increased fluidity because of the high welding heat. Thus, the molten filler could more easily spread to fill the through holes at a high welding power than at a low welding power [31]. Mg alloys possess lower melting temperatures than Al, and they are highly reactive at elevated temperatures [31].

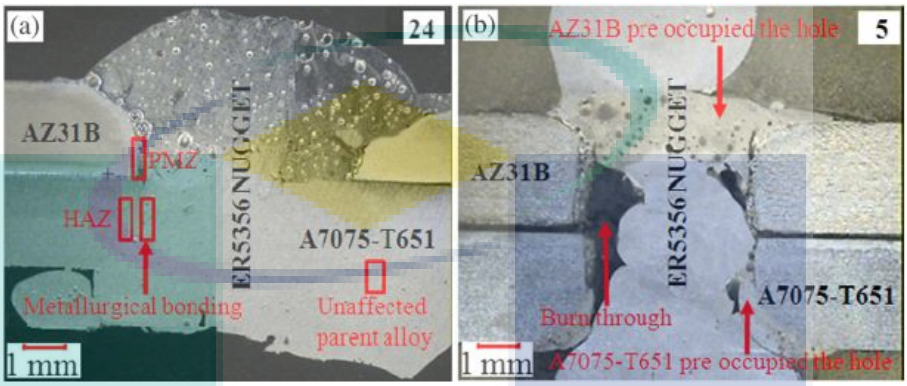

Fig. 4.3. Welding macro cross sections. a) With complete nugget. b) With incomplete nugget

Therefore, some materials around the through holes on the AZ31B parent alloy side melted and occupied the spaces in the through holes during welding. Initiating the arc welding at the hole periphery rather than at the center of the holes is the cause of this occurrence. However, this condition is an uncontrollable incident in welding and is probably another reason why some nuggets were not fully constructed in the intervening layers. Some burn-throughs were also observed in the welding cross sections with incomplete nuggets; thus, the fillers could not fill the gaps in these sections. The welding macro cross sections of the joints with complete and incomplete nuggets are shown in Fig. 4.3a, b.

Al and Mg alloys also possess low solubility in each other [23, 32]. Therefore, the presence of any metallurgical bonding between the filler and AZ31B alloy in the welding joints cannot be definitively determined by macrostructural observation alone. However, a certain metallurgical bonding is believed to be present between the Al nuggets and AZ31B parent alloy. In the welding joints between any Al and Mg alloys with any Al filler, the formation of brittle AlmMgn IMCs is a common phenomenon. SEM and EDX analyses were performed to investigate the mechanisms of metallurgical bonding and the formation of AlmMgn IMCs in the welding joints, and details of which

are described in Section 3.5. Fig.. 4.4 shows the microstructures at different locations of the welding cross sections shown in Fig. 4.3a, b.

The microstructures in the welding cross sections are shown in Fig. 4.4a–e. Fig. 4.4a,c show the microstructure on the A7075-T651 alloy side. Figure 4b, d show the microstructure on the AZ31B alloy side. Figure 4.4e shows the overall microstructure of the Al nugget. Two types of microstructures of the A7075-T651 alloy were observed. The microstructure of the unaffected A7075-T651 parent alloy is shown in Fig. 4.4a, and that of the PMZ is shown in Fig. 4.4b. The HAZ was not distinguishable or might have existed along with PMZ. Thus, the HAZ was not shown in the figure. The grains in the microstructure of the PMZ of the A7075-T651 alloy recrystallized; thus, the grains increased in size. The grain boundary became shaggy compared with that of the parent alloy because of the effects of welding heat. The microstructure showed that the grains in the PMZ of the A70750-T651 alloy were equiaxed. The PMZ contained some microvoids and most probably minute amounts of AlmFen and AlnMnm compounds.

By contrast, two microstructures were observed on the AZ31B alloy side: those of the unaffected AZ31B parent alloy, as shown in Fig. 4.4b, and the PMZ of the AZ31B alloy. The HAZ might have existed along with the PMZ and was unapparent. The microstructure of the PMZ was coarser than that of the parent alloy because of the effect of the welding heat. The grayish-black phases in the PMZ on the AZ31B alloy side were probably MgZn2 and Al6Mg11Zn11 compounds in accordance with the element compositions of the AZ31B parent alloy and ER5356 Al filler [33]. Some large microvoids were also observed. The microstructures of the ER5356 Al nugget showed almost the same features throughout the entire nugget area, with minimal differences in grain sizes. This condition might be due to different cooling rates at different parts of the Al nugget at the time of solidification. As shown in Fig. 4.4e, the dendrites were dominant in the Al nugget, and some equiaxed dendrites also existed.

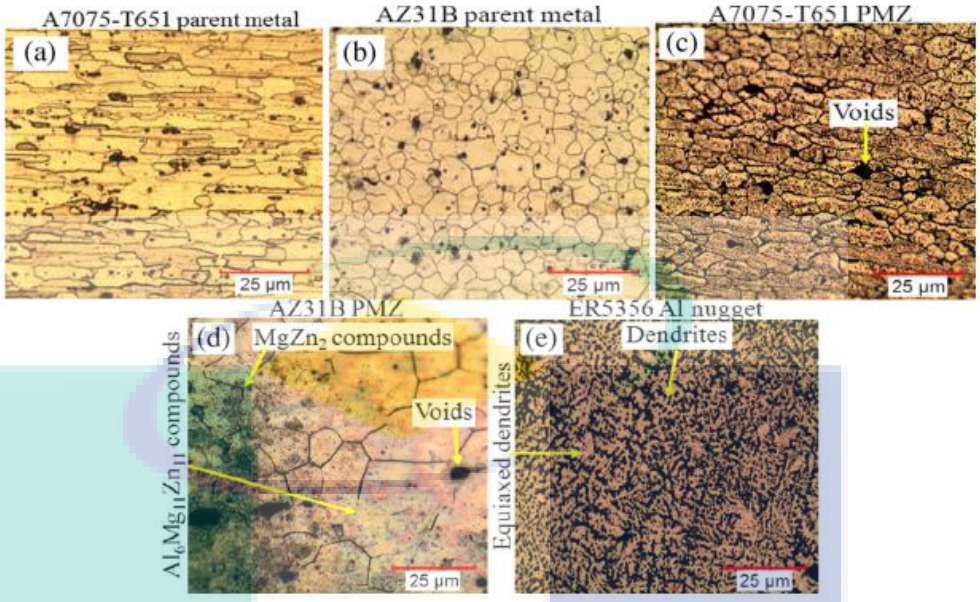

Fig. 4.4. Microstructure at welding cross section a) at A7075-T651 parent alloy, b) at AZ31B parent alloy, c) at PMZ of A7075-T651 alloy, d) at PMZ of AZ31B alloy, and e at Al nugget.

4.4.3 Location of Failure

Two types of fractures occurred during tensile and impact toughness testing. During tensile testing, 25 joints fractured in the Al nugget, and only 1 joint fractured in the AZ31B parent alloy. During impact toughness testing, 16 joints fractured in the Al nugget and 10 joints fractured in the AZ31B parent alloy. The fracture surface morphologies in the different fracture locations were investigated by SEM and analyzed by EDX to reveal the facts and features of the fracture in the AZ31B alloy and Al nugget, and details of which are discussed in Section 4.3.4. The fracture locations of all joints during tensile and toughness testing are listed in Table 4.3.

Table 4.3. Location of fracture for tensile and charpy test

Exp. No.	ER5356 Al filler	
	Fracture location	
	Tensile Test	Toughness Test
1	N	M
2	N	N
3	N	M
4	N	N
5	N	N
6	M	M
7	N	N
8	N	N

9	N	M
10	N	N
11	N	N
12	N	N
13	N	M
14	N	N
15	N	M
16	N	N
17	N	N
18	N	N
19	N	N
20	N	N
21	N	N
22	N	M
23	N	N
24	N	M
25	N	M
26	N	N

4.4.4 Fracture Surface Morphology

The SEM images of the fracture surface of the AZ31B alloy during tensile and toughness testing are shown in Fig. 4.5. The fracture surface of the unaffected AZ31B parent alloy was composed of cleavage planes, cleavage steps, and cloudy dimples. The cleavage planes were small, and the cleavage rivers were short and unapparent. Few inherent microvoids and cracks were also present. The fracture surface in the PMZ of the AZ31B alloy contained large microvoids, micropores, cracks, and oxides. The AZ31B alloy exhibited more sensitivity to the welding heat; as a result, pores, voids, cracks, and oxidation occurred in this alloy. As shown in Fig. 4.5, the fracture surface in the PMZ of the AZ31B alloy side contained some oxides that were introduced during welding because of the strong affinity of Mg to oxygen.

The presence of pores has detrimental effects on the ductility of materials and is one of the causes of cracks and brittle fractures, which commonly occur during Mg welding [8]. Oxides promote the formation of more cracks and reduce bending elongation. Thus, during tensile and toughness testing, the pores, cracks, and oxides introduced during welding were broken up further and distributed in a scattered mode. The formation of brittle AlmMgn IMCs is normal on the AZ31B alloy side if welded with an Al-based filler. These IMCs reduce the effective loadbearing area [34, 35]. During tensile and toughness testing, the inconsistent deformation of AlmMgn IMCs and oxides in the PMZ along with the inherent microvoids, micropores, and

microcracks caused stress concentrations in the matrices and combined to form large cracks. As a result, the AZ31B alloy was affected more severely than the A7075-T651 alloy and ER5356 Al nugget by the pores, cracks, oxides, and brittle AlmMgn IMCs. This condition easily promoted crack propagation in the AZ31B alloy during tensile and toughness testing; as a result, fracture occurred in this alloy.

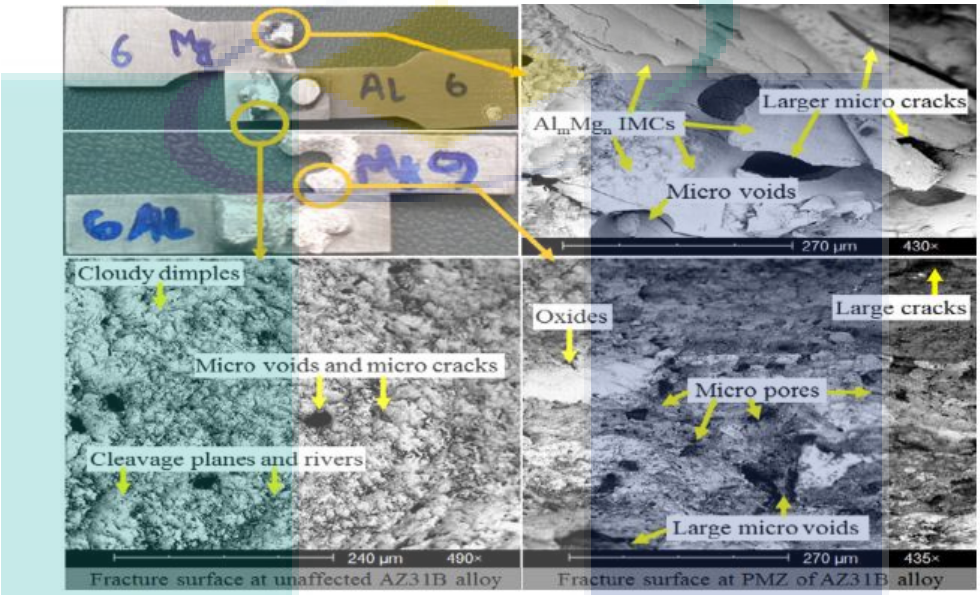

Fig. 4.5. SEM images of fracture surface at AZ31B alloy

EDX analysis was performed at different fracture surface locations in the PMZ of the AZ31B alloy to determine the facts and features of the fracture in the zone, as shown in Fig. 4.6. Table 4.4 shows graphically and numerically the atomic percentages of the elements at points 1, 2, and 3 of the fracture surface in the PMZ of the AZ31B alloy. The analysis revealed that the fracture surface of AZ31B alloy mainly contained Mg (96.167 %), Al (2.050 %), Mn (1.462 %), Zn (0.283 %), Si (0.028 %), Ca (0.006 %), and Fe (0.005 %). These elements are the alloying elements normally present in the AZ31B alloy. The main elements in this zone were Mg, O, and Al. Al and Mg were mainly from the ER5356 Al filler and AZ31B parent alloy, respectively. The atomic percentages of Mg were 69.394 and 50.186 % at points 2 and 3, respectively. The atomic percentages of Al were 9.538 and 48.336 % at points 2 and 3, respectively. The atomic percentage of O was 19.673 % at point 2.

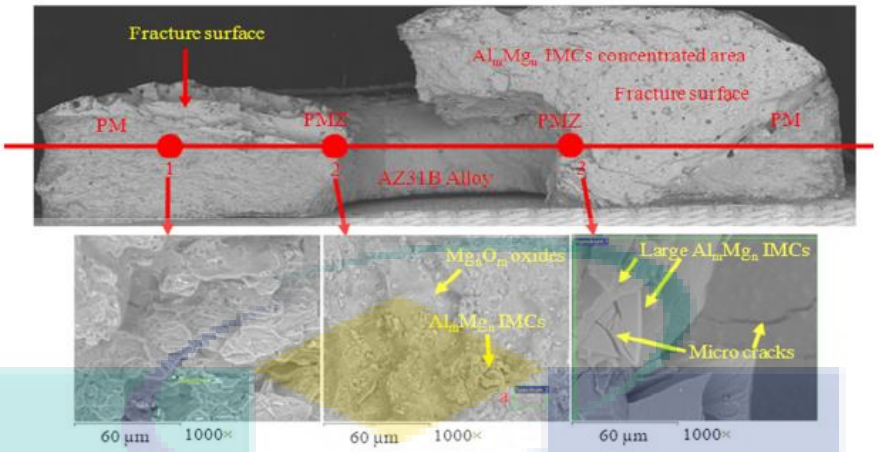

Fig. 4.6. EDX at different locations of AZ31B alloy fracture surface (with Al filler)

Table 4.4. EDX results of unaffected AZ31B alloy (point 1) and AZ31B alloy PMZ (point 2 and point 3) fracture surface

Elements	**Atomic %**		
	Point 1	**Point 2**	**Point 3**
Magnesium	960167	69.394	50.186
Oxygen	-	19.673	-
Aluminium	2.050	9.538	48.336
Silicon	0.028	-	-
Calcium	0.006	-	0.151
Manganese	1.462	0.120	-
Iron	0.005	-	0.162
Zinc	0.283	-	0.656
Sodium	-	0.378	-
Gallium	-	0.304	-
Titanium	-	-	0.228
Chromium	-	-	0.170
Nickel	-	-	0.11

Therefore, the element analysis results showed that good amounts of AlmMgn IMCs and magnesium oxide (MgnOm) were present in the PMZ of the AZ31B alloy, thereby causing the fracture on the AZ31B alloy side. Fig. 4.7 shows the SEM images of the fracture surface of the ER5356 Al nugget. The failure occurring in the Al nuggets was caused by the incomplete formation of nuggets in the intervening layers during double sided welding, as shown in Fig. 4.3b. The diffusion of some melted AZ31B alloy in the intervening layers of the nugget also caused the formation of a large amount of brittle AlmMgn IMCs [36]. Moreover, large microvoids, cracks, aluminum oxides (AlmOn), and MgnOm were also present, causing crack initiation. As a result, the propagation of large cracks occurred during tensile and toughness testing. Furthermore, a highly brittle fracture mechanism was present in the core of the Al nuggets because of

the formation of large voids, cracks, oxides, and a large amount of AlmMgn IMCs. These factors combined with the incomplete formation of some nuggets, resulting in the relative weakness of the Al nuggets compared with the A7075-T651 and AZ31B alloys and the fracture in the Al nugget.

Table 4.5 graphically and numerically shows the atomic percentages of the elements at two points of the fracture surface of the Al nugget. The EDX analysis locations at point 1 and 2 are shown in Fig. 4.8. The main elements in this zone were Al, Mg, and O. Al and Mg clearly originated from the ER5356 Al filler and AZ31B parent alloy, respectively. The atomic percentages of the elements were as follows: 53.327 % (Al), 24.859 % (O), and 21.332 % (Mg) at point 1; 62.921 % (Al), 31.856 % (Mg), and 4.774 % (O) at point 2. Therefore, as shown in the element analysis, good amounts of brittle AlmMgn IMCs, AlmOn, and MgnOm formed in the intervening layers of an Al nugget. MgnOm resembled a blister. Some macrovoids also formed. The macrovoids, AlmMgn IMCs, and oxides stimulated the formation and propagation of large cracks in the ER5356 Al nuggets during tensile and toughness testing, thereby causing a fracture.

Table 4.5 EDX analysis at point 1 and point 2 of A7075-T651/Al nugget bonding

Elements	Atomic %	
	Point 1	Point 2
Carbon	24.859	4.774
Oxygen	21.332	31.856
Magnesium	53.327	62.921
Aluminium	0.136	0.037
Zinc	0.346	0.412

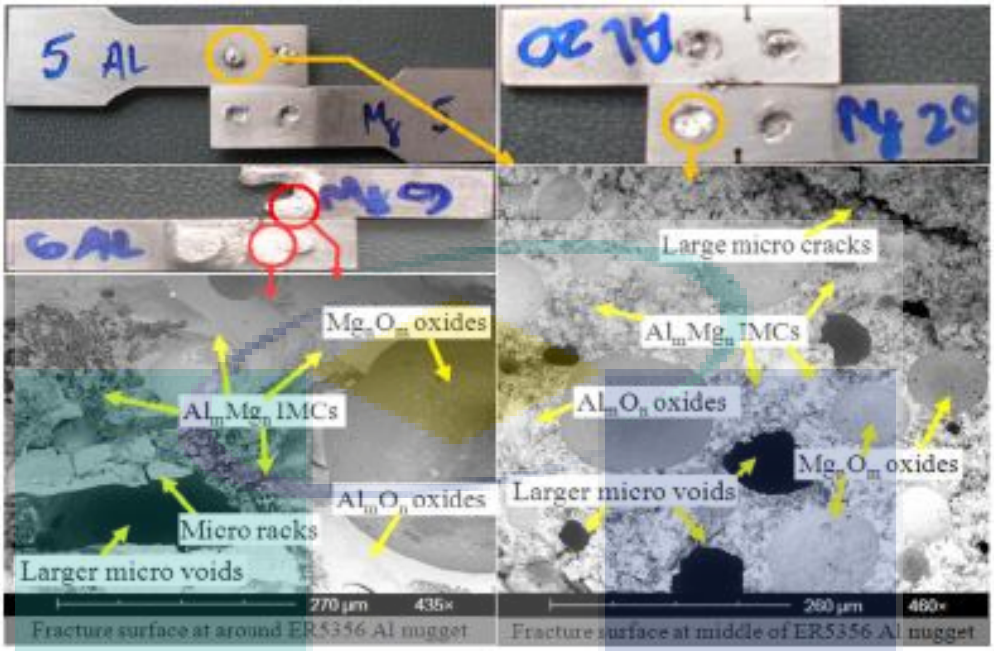

Fig. 4.7. SEM images of fracture surface at ER5356 Al nugget.

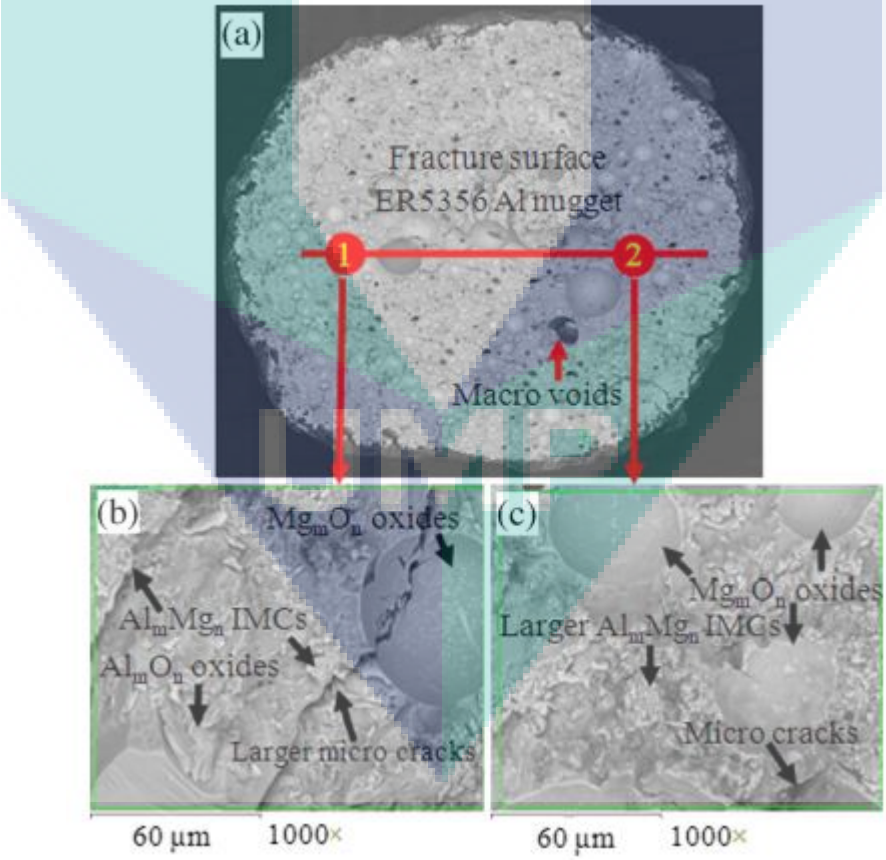

Fig. 4.8. EDX analysis at fracture surface at ER5356 Al nugget.

4.4.5 EDX Analysis on Metallurgical Bonding

The welding cross section shown in Fig. 4.9 presents the metallurgical bonding between the parent alloys and ER5356 Al nugget. The bonding between the AZ31B alloy and Al nugget, which was approximately 20–40-µm thick, was rugged. By contrast, the bonding between A7075-T651 alloy and Al nugget was very smooth and thin, measuring approximately 2– 3-µm thick. Table 4.6 presents the EDX-derived atomic percentages of the elements at points 1 and 2 of the AZ31B/Al nugget bonding.

Table 4.6. EDX analysis at point 1 and point 2 at AZ31B/ER5356 Al nugget bonding and at ER5356 Al nugget/AZ31B alloys bondiung respectively

Elements	Atomic %	
	Point 1	Point 2
Oxygen	-	28.119
Magnesium	55.336	50.117
Aluminium	40.981	18.732
Silicon	1.314	0.49
Zinc	1.146	0.32
Calcium	0.915	0.924
Manganese	0.199	0.333
Iron	-	0.295
Nickel	-	0.617

The EDX analysis results revealed that the AZ31B/ Al bonding mostly contained Mg, Al, O, Si, and Zn. The Mg elements were from the AZ31B alloy, whereas the Al, Si, and were introduced during welding. Numerous macropores were present in the Al nugget on the AZ31B side. Based on the EDX analysis results on the atomic percentages of the elements, a large amount of AlmMgn IMCs and minute amounts of AlmOn and MgnOm were present in the bonding. Table 4.7 presents the EDX-derived atomic percentages of the elements at points 1 and 2 of the A7075-T651/Al nugget bonding. The A7075-T651/Al nugget bonding mostly contained Al, C, Mg, and O. Al was from both the A7075- which was approximately 20–40-µm thick, was rugged. By contrast, the bonding between A7075-T651 alloy and Al nugget was very smooth and thin, measuring approximately 2– 3-µm thick. Table 4.6 presents the EDX-derived atomic percentages of the elements at points 1 and 2 of the AZ31B/Al nugget bonding. The EDX analysis results revealed that the AZ31B/ Al bonding mostly contained Mg, Al, O, Si, and Zn. The Mg elements were from the AZ31B alloy, whereas the Al, Si, and Zn elements were definitely from the Al filler. The O elements

were introduced during welding. Numerous macropores were present in the Al nugget on the AZ31B side. Based on the EDX analysis results on the atomic percentages of the elements, a large amount of AlmMgn IMCs and minute amounts of AlmOn and MgnOm were present in the bonding.

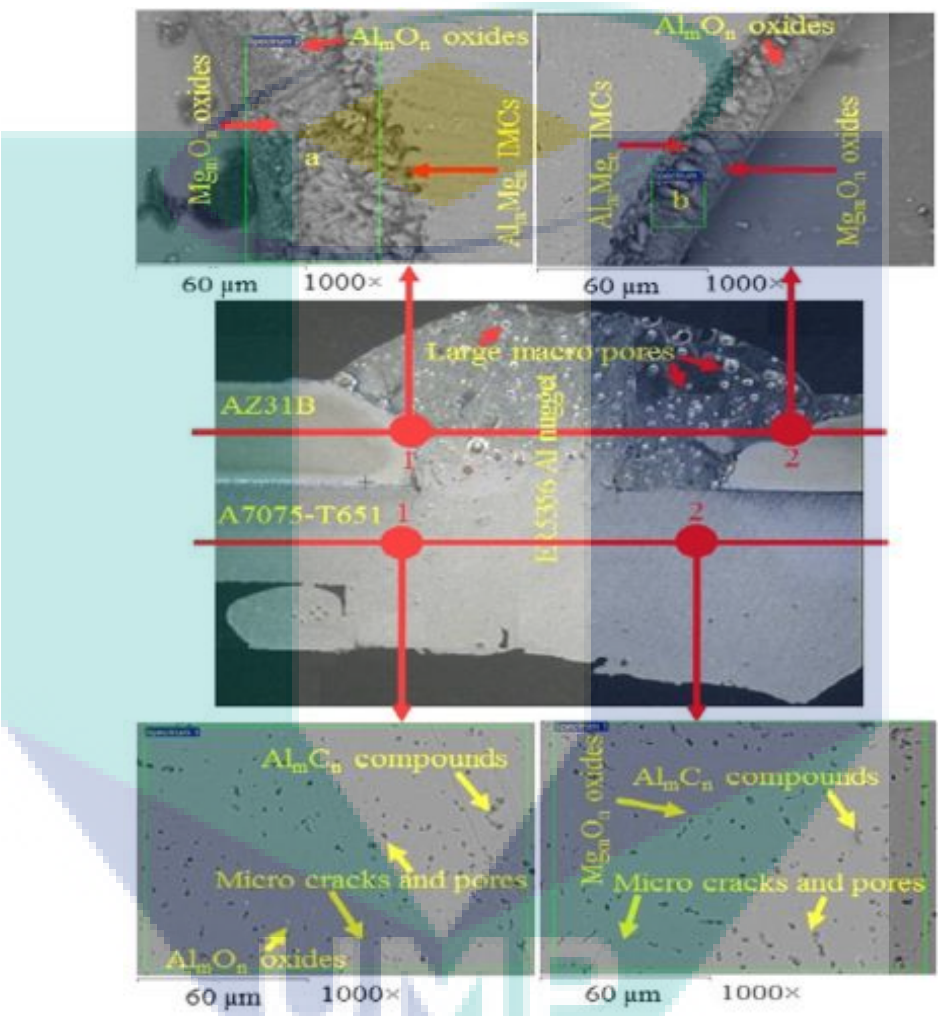

Fig. 4.9. EDX at AZ31B/ER5356 nugget and A7075-T651/ER5356 nugget bonding

Table 4.7 presents the EDX-derived atomic percentages of the elements at points 1 and 2 of the A7075-T651/Al nugget bonding. The A7075-T651/Al nugget bonding mostly contained Al, C, Mg, and O. Al was from both the A7075- T651 parent alloy and ER5356 Al filler. Mg was from the ER5356 Al filler, which had a high Mg content (~5 %). C and O elements were introduced during welding. According to the atomic ratio, minute amounts of aluminum carbide (AlmCn) compounds, AlmOn, and MgnOm were present in the A7075-T651/Al nugget bonding. Few microcracks and micropores

were also present. No fracture occurred in either the AZ31B/Al nugget or the A7075-T651/Al nugget bonding during tensile and toughness testing.

Table 4.7. EDX analysis at point 1 and point 2 of A7075-T651/Al nugget bonding

Elements	Atomic %	
	Point 1	Point 2
Carbon	18.011	17.085
Oxygen	3.166	2.268
Magnesium	4.334	4.469
Aluminium	73.427	75.844
Zinc	0.103	0.149

4.5 CONCLUSIONS

i. A7075-T651 and AZ31B dissimilar alloys were successfully lap-welded by a new technique called GMA plug welding method using an ER5356 Al filler. Significantly improved mechanical properties were achieved. The welding parameters 15 L/min GSR, 8 mm TWD, 15 V WV, and 115 AWC were considered optimal because they allowed for the highest tensile strength and a good impact toughness. The maximum YS, UTS, and impact toughness of the joints were 97.830 MPa, 226.28 MPa (89 % of the UTS of the AZ31B parent alloy), and 7.42 J (84 % of the impact toughness of the AZ31B parent alloy), respectively. Therefore, the objective of achieving significantly enhanced mechanical properties of the joint by reducing the direct bonding area between A7075-T651 and AZ31B alloys by using the ER5356 Al filler was satisfied by the proposed GMA plug welding method.

ii. Although most nuggets were fully constructed, filling the spaces in the through holes in the A7075-T651 and AZ31B parent alloys, some nuggets were not. This condition occurred because of the differences in the viscosity and fluidity levels of the molten fillers at different welding powers. Certain AZ31B materials melted and occupied the spaces in the through holes during welding given that Mg alloys have lower melting temperatures than Al. Initiating the arc welding at the hole periphery rather than at the center of the holes was the reason for this occurrence. Some burn-throughs were also observed in the welding cross sections with incomplete nuggets. The grains in the microstructure of the PMZs of the A7075- T651 and AZ31B alloys were recrystallized; as a result, the grains increased in size, and the grain boundary became shaggy compared with that of the parent alloy because of the effects of the welding heat. The grains in the microstructure of the PMZ of the A70750-T651 alloy were equiaxed, and

this PMZ might have contained minute amounts of Al mFen and AlnMnm compounds along with some microvoids. The grayish-black phases in the PMZ on the AZ31B alloy side were probably MgZn2 and Al6Mg11Zn11 compounds. Some large microvoids were observed. The microstructures of the ER5356 Al nugget showed almost the same features throughout the entire nugget area.

iii. A total of 25 joints failed in the Al nugget, and only 1 joint failed in the AZ31B parent alloy during tensile testing. A total of 16 joints failed in the Al nugget and 10 joints failed in the AZ31B parent alloy during impact toughness testing. Most of the failures occurred in the Al nugget because cracks initiated as a result of the large amounts of AlmOn, MgnOm, and brittle AlmMgn IMCs; micropores; voids; and cracks. No joints failed in the A7075-T651 parent alloy. The EDX analysis results revealed that a fair amount of Al mMgn IMCs were observed in the cross sections of the joints especially between the Al nugget and the AZ31B parent alloy. However, the amount was definitely significantly lower than that generated by other welding techniques because the bonding area between A7075-T651 and AZ31B dissimilar alloys was less in the proposed technique. Therefore, the joints formed by the proposed technique showed better mechanical performance (strength and toughness) than those by other welding techniques.

iv. The thickness of the AZ31B/Al nugget bonding and that of the A7075-T651/Al nugget bonding were approximately 2–3 μm and 20–40 μm, respectively. These layers mostly contained brittle AlmMgn IMCs, AlmOn, MgnOm, AlmCn compounds, and some micropores and voids. No evidence of fracture occurring in these bonding areas could be revealed by tensile and toughness testing.

4.6 REFERENCE

[1] Karunakaran N, Balasubramanian V (2011) Effect of pulsed current on temperature distribution, weld bead profiles and characteristics of gas tungsten arc welded aluminum alloy joints. Trans Nonferrous Metals Soc China 21(2):278–286. doi:10.1016/s1003-6326(11)60710-32.

[2] Hayat F (2011) The effects of the welding current on heat input, nugget geometry, and the mechanical and fractural properties of resistance spot welding on Mg/Al dissimilar materials. Mater Des 32(4):2476–2484

[3] Zhang HT, Song JQ (2011) Microstructural evolution of aluminum/ magnesium lap joints welded using MIG process with zinc foil as an interlayer. Mater Lett 65(21–22):3292–3294. doi:10.1016/j.matlet.2011.05.080

[4] X-d Q, L-m L (2012) Fusion welding of Fe-added lap joints between AZ31B magnesium alloy and 6061 aluminum alloy by hybrid laser–tungsten inert gas welding technique. Mater Des 33:436–443

[5] Yan YB, Zhang ZW, Shen W, Wang JH, Zhang LK, Chin BA (2010) Microstructure and properties of magnesium AZ31B– Table 7 EDX analysis at point 1 and point 2 of A7075-T651/Al nugget bonding Elements Atomic % Point 1 Point 2 Carbon 18.011 17.085 Oxygen 3.166 2.268 Magnesium 4.334 4.469 Aluminum 73.427 75.844 Zinc 0.103 0.149 2782 Int J Adv Manuf Technol (2017) 88:2773–2783 aluminum 7075 explosively welded composite plate. Mater Sci Eng A 527(9):2241–2245. doi:10.1016/j.msea.2009.12.007

[6] Pieta G, dos Santos J, Strohaecker T, Clarke T (2013) Optimization of friction spot welding process parameters for AA2198-T8 sheets. Mater Manuf Process 29(8):934–940, just-accepted

[7] Hu H, Yu A, Li N, Allison JE (2003) Potential magnesium alloys for high temperature die cast automotive applications: a review. Mater Manuf Process 18(5):687–717

[8] Mofid M, Abdollah-Zadeh A, Malek Ghaini F (2012) The effect of water cooling during dissimilar friction stir welding of Al alloy to Mg alloy. Mater Des 36:161–167

[9] Chen Y, Nakata K (2008) Friction stir lap joining aluminum and magnesium alloys. Scr Mater 58(6):433–436 10. Kwon Y, Shigematsu I, Saito N (2008) Dissimilar friction stir welding between magnesium and aluminum alloys. Mater Lett 62(23):3827–3829

[10] Liu C, Chen D, Bhole S, Cao X, Jahazi M (2009) Polishing-assisted galvanic corrosion in the dissimilar friction stir welded joint of AZ31 magnesium alloy to 2024 aluminum alloy. Mater Charact 60(5):370–376

[12] Chen YC, Nakata K (2008) Friction stir lap joining aluminum and magnesium alloys. Scr Mater 58(6):433–436. doi:10.1016/j.scriptamat.2007.10.033

[13] Mofid MA, Abdollah-zadeh A, Malek Ghaini F (2012) The effect of water cooling during dissimilar friction stir welding of Al alloy to Mg alloy. Mater Des 36:161–167.doi:10.1016/j.matdes.2011.11.004

[14] Casalino G (2007) Statistical analysis of MIG-laser CO2 hybrid welding of Al–Mg alloy. J Mater Process Technol 191(1–3):106–110. doi:10.1016/j.jmatprotec.2007.03.065

[15] Chang W-S, Rajesh S, Chun C-K, Kim H-J (2011) Microstructure and mechanical properties of hybrid laser-friction stir welding between AA6061-T6 Al alloy and AZ31 Mg alloy. J Mater Sci Technol 27(3):199–204

[16] Yan J, Xu Z, Li Z, Li L, Yang S (2005) Microstructure characteristics and performance of dissimilar welds between magnesium alloy and aluminum formed by friction stirring. Scr Mater 53(5):585–589

[17] Shang J, Wang K, Zhou Q, Zhang D, Huang J, Li G (2012) Microstructure characteristics and mechanical properties of cold metal transfer welding Mg/Al dissimilar metals. Mater Des 34:559–565

[18] Yan Y, Zhang Z, Shen W, Wang J, Zhang L, Chin B (2010) Microstructure and properties of magnesium AZ31B–aluminum 7075 explosively welded composite plate. Mater Sci Eng A 527(9):2241–2245

[19] Liu X-H, Gu S-H, Wu R-Z, Leng X-S, Yan J-C, Zhang M-L (2011) Microstructure and mechanical properties of Mg-Li alloy after TIG welding. Trans Nonferrous Metals Soc China 21(3):477–481

[20] Tabasi M, Farahani M, Givi MKB, Farzami M, Moharami A (2015) Dissimilar friction stir welding of 7075 aluminum alloy to AZ31 magnesium alloy using SiC nanoparticles. Int J Adv Manuf Technol. doi:10.1007/s00170-015-8211-y, 1–11

[21] Pokataev E, Trykov YP (2004) Residual stresses in magnesium–aluminium composites, produced by explosive welding. Weld Int 18(8):656–659

[22] Carlone P, Astarita A, Palazzo GS, Paradiso V, Squillace A (2015) Microstructural aspects in Al–Cu dissimilar joining by FSW. Int J Adv Manuf Technol 79(5):1109–1116. doi:10.1007/s00170-015-6874-z

[23] Zhang H, Song J (2011) Microstructural evolution of aluminum/ magnesium lap joints welded using MIG process with zinc foil as an interlayer. Mater Lett 65(21):3292–3294

[24] Ishak M, Maekawa K, Yamasaki K (2012) The characteristics of laser welded magnesium alloy using silver nanoparticles as insert material. Mater Sci Eng A 536:143–151

[25] Cao R, Wen B, Chen J, Wang P-C (2013) Cold metal transfer joining of magnesium AZ31B-to-aluminum A6061-T6. Mater Sci Eng A 560:256–266

[26] Temmar M, Hadji M, Sahraoui T (2011) Effect of post-weld aging treatment on mechanical properties of tungsten inert gas welded low thickness 7075 aluminium alloy joints. Mater Des 32(6): 3532–3536. doi:10.1016/j.matdes.2011.02.011

[27] Tarpani JR, Maluf O, Gatti MCA (2009) Charpy impact toughness of conventional and advanced composite laminates for aircraft construction. Mater Res 12(4):395–403

[28] Erturk MT (2011) Microstructural and mechanical characterization of metal active gas welded joint between cast iron and low carbon steel. Master's Thesis, Middle East Technical University
[29] Padmanaban G, Balasubramanian V (2011) Effects of laser beam welding parameters on mechanical properties and microstructure of AZ31B magnesium alloy. Trans Nonferrous Metals Soc China 21(9):1917–1924
[30] Simoncini M, Forcellese A (2012) Effect of the welding parameters and tool configuration on micro- and macro-mechanical properties of similar and dissimilar FSWed joints in AA5754 and AZ31 thin sheets. Mater Des 41:50–60
[31] Hirano S, Okamoto K, Doi M, Kamura O, Inagaki M, Aono Y (2004) Microstructure of the interface in magnesium alloy to aluminium alloy dissimilar joints produced by friction stir welding. Weld Int 18(9):702–708
[32] Miao Y, Han D, Yao J, Li F (2010) Effect of laser offsets on joint performance of laser penetration brazing for magnesium alloy and steel. Mater Des 31(6):3121–3126
[33] Liu F, Ren D, Liu L (2013) Effect of Al foils interlayer on microstructures and mechanical properties of Mg–Al butt joints welded by gas tungsten arc welding filling with Zn filler metal. MaterDes46:419–425
[34] Li J-F, Z-w P, Li C-X, Jia Z-Q, W-j C, Zheng Z-Q (2008) Mechanical properties, corrosion behaviors and microstructures of 7075 aluminium alloy with various aging treatments. Trans Nonferrous Metals Soc China 18(4):755–762
[35] Liu F, Wang H, Liu L (2014) Characterization of Mg/Al butt joints welded by gas tungsten arc filling with Zn–29.5 Al–0.5 Ti filler metal. Mater Charact 90:1–6
[36] Liu L, Ren D (2011) A novel weld-bonding hybrid process for joining Mg alloy and Al alloy. Mater Des 32(7):3730–3735

CHAPTER 5

CONCLUSION AND RECOMENDATION

5.1 Conclusion

The experimental and numerical methodology results from this project showed that the orientation state of the art of joining dissimilar metals between aluminium and magnesium alloys is highly depends on the welding method. This research deals with the approach of shoulder to pin ratio of magnesium alloy AZ31 by using Friction stir welding. Instead of parameter optimization, the effect of parameter, mathematical model and metallurgical analysis were conducted to fulfil the research purpose. In addition, the significant outcomes from the research work followed by recommendation for the next improvement in welding AZ31B Mg alloys using low power fiber laser machine also summarized.

For the dissimilar welding by MIG plug weld method of Al 7075 and AZ31B, the weld was successfully done. Better mechanical properties were achieved with SS filler comparing to Al filler. The experiments for models validation showed that the models have high accuracy in predicting the responses as the errors are much less than 8%. A7075-T651/SS nugget and AZ31B/SS nugget metallurgical bonding were discontinuous and were about the size of 2 to 5 µm thick. AZ31B/SS nugget bonding area contained Fe_mO_n oxides, Fe_mC_n compounds and little Fe-Al, Fe-Mg IMCs. A7075-T651/SS nugget bonding contained Fe_mC_n compounds and Fe-Al IMCs. Both the bonding contained macro and micro voids. No evidence could be revealed for any fracture initiation from these bonding at the time of tensile and toughness testing. On the other hand, AZ31B/Al nugget and A7075-T651/Al nugget bonding were the size of 20 to 40 µm and 2 to 3 µm respectively. These layers mostly contained Al_mMg_n brittle IMCs, Al_mO_n and Mg_nO_m oxides, Al_mC_n compounds, some micro pores and voids. No

evidence of fracture occurring from these bonding could be revealed in tensile and toughness testing.

5.2 Recommendation for future work

The mechanical properties, modeling and metallurgical properties of the lap welded joint between A7075-T651 and AZ31B alloys by new technique of GMA plug welding method have been studied. The more successful application of this method of welding can be expanded by the recommended further research below:

- The better metallurgical bonding between ER308L-Si SS/A7075-T651 and ER308L-Si SS/AZ31B through after heat treatment of the joint can improve both mechanical and metallurgical properties of the joint. The proper and effective method for the heat treatment can be a feasible future research.
- Pouring liquid steel into the through holes to form nugget to join these two high profile dissimilar alloys can also be attempted. The study of bonding method and mechanism of Al and Mg alloys to steel through the solubility phenomena can also be a vital part of further research.
- The butt welding joint between A7075-T651 and AZ31B alloys or between other Al/Mg alloys using non Al or non-Mg based filler wire with nearly similar physical, chemical and mechanical properties to Al and Mg alloys (Like Zn based filler wire) can also be a topic for future research.

CHAPTER 6

RESEARCH OUTPUT

6.1 List of Published Papers

1. M Ishak, MR Islam, T Sawa (2014), *GMA spot welding of A7075-T651/AZ31B dissimilar alloys using stainless steel filler*, Materials and Manufacturing Processes 29 (8), 980-987.
2. M Ishak, MR Islam (2014), *Weldability of A7075-T651 and AZ31B dissimilar alloys by MIG welding method based on welding appearances*, Journal of Physics: Conference Series 495 (1), 012022.
3. M Islam (2014), *Modelling and Optimizing of Joint's Fracture Toughness between A7075-T651 and AZ31B Dissimilar Alloys Welded by GMA Spot Welding Method*, Applied Mechanics and Materials 663, 281-286.
4. NH Othman, LH Shah, M Ishak (2015), *Mechanical and microstructural characterization of single and double pass Aluminum AA6061 friction stir weld joints*, IOP Conference Series: Materials Science and Engineering 100 (1), 012016.
5. MNM Salleh, M Ishak, LH Shah, SRA Idris (2016), *The effect of ER4043 and ER5356 filler metal on welded Al 7075 by metal inert gas welding*, High Performance and Optimum Design of Structures and Materials II 166, 213.
6. MNM Salleh, M Ishak, FRM Romlay, MH Aiman (2016), *A study on bead-on-plate welding of AA7075 using low power fiber laser*, Journal of Mechanical Engineering and Sciences 10 (2), 2065-2075.
7. NH Othman, N Udin, M Ishak, LH Shah (2016), *Effect of Taper Pin Ratio on Microstructure and Mechanical Property of Friction Stir Welded AZ31 Magnesium Alloy, World Academy of Science, Engineering and Technology, International Journal of Chemical, Molecular, Nuclear*, Materials and Metallurgical Engineering, 10(5), pp. 638-641.
8. NH Othman, N Abdul Razak, LH Ahmad Shah, M Ishak (2016), *Effect of Taper Pin Ratio on AA7075 Aluminium Alloy Friction Stir Welding*, Key Engineering Materials 701, 154-158.
9. MR Islam, M Ishak, LH Shah, SRA Idris, C Meriç (2017), *Dissimilar welding of A7075-T651 and AZ31B alloys by gas metal arc plug welding method*, The

International Journal of Advanced Manufacturing Technology 88 (9-12) pp. 2773-2783.

10. NH Othman, M Ishak, LH Shah (2017*), Effect of shoulder to pin ratio on magnesium alloy Friction Stir Welding*, IOP Conference Series: Materials Science and Engineering 238 (1), 012008.
11. MNM Salleh, M Ishak, MH Aiman, SRA Idris, FRM Romlay (2017), *Investigation on the Effect of Pulsed Energy on Strength of Fillet Lap Laser Welded AZ31B Magnesium Alloys*, IOP Conference Series: Materials Science and Engineering 238 (1), 012009.
12. M ISHAK, MNM SALLEH, SR AISHA (2017), *The Mechanical And Microstructural Study Of Welded Aa7075 Using Different Filler Metals*, International Journal of Computational Methods and Experimental Measurements, 5 (5), pp. 696-712.
13. NM Salleh, M Ishak, FR Romlay (2017*), Effect of fiber laser parameters on laser welded AZ31B Magnesium alloys*, MATEC Web of Conferences 90, 01032.

6.2 List of Conferences

1. A study on bead-on-plate welding of AA7075 using low power fiber laser, 3rd International Conference of Mechanical Engineering Research (ICMER), August 2015, Zenith, Kuantan, Malaysia.
2. Lap joint dissimilar welding of aluminium AA6061 and galvanized iron using TIG welding, 3rd International Conference of Mechanical Engineering Research (ICMER), August 2015, Zenith, Kuantan.
3. Effect of fiber laser parameters on laser welded AZ31B Magnesium alloys, 2nd International Conference on Automotive Innovation & Green Energy Vehicle (AiGEV) August 2016, Malaysian Automotive Institute, Cyberjaya., Malaysia.
4. Investigation on the Effect of Pulsed Energy on Strength of Fillet Lap Laser Welded AZ31B Magnesium Alloys, Joining and Welding Sympossium, July 2017, UMP, Pekan, Malaysia.
5. Effect of shoulder to pin ratio on magnesium alloy Friction Stir Welding, Joining and Welding Sympossium, July 2017, UMP, Pekan, Malaysia.

6. Double Fillet Lap of Laser Welding of Thin Sheet AZ31B Mg Alloy, International Laser Technology and Optics Sympossium (iLATOS), September 2017, Pulai Spring Resort, Skudai, Johor Bharu.

6.3 List of Exhibitions

1. Dissimilar Aluminium Alloy A7075 and A6061 Welding Technique, Creation Innovation Technology and Research Exposition (CITREX) 2015 on 9 – 10th March, Silver Medal Award.
2. A Novel Design of Backing Plate and Clamping System for Dissimilar Friction Stir Welding, Creation Innovation Technology and Research Exposition (CITREX) 2017 on 15-16th of March, Bronze Medal Award.

APPENDICES

OTHER RELATED PUBLISHED WORKS

1. Effect of fiber laser parameters on laser welded AZ31B Magnesium Alloys

(Matec Web of Conference 90, 01032 (2017))

Abstract: Recently, the usage of AZ31B had been hugely applied in the industrial application such as in automotive, marine, electronic, and also packaging purposes due to its advantage of recyclability and lightweight. Magnesium alloys required low heat input to be weld since the elements were easily evaporated because this metal possesses lower melting point. Laser welding application was more convenient to weld magnesium alloys due to its high power and lower heat input. AZ31B was selected since it has strong mechanical properties among other Mg alloys due to the major alloying elements are Aluminium and Zinc. Low power fibre laser machine with wavelength 900 nm was used in this experiment. The intention of this work was to

investigate the effect of low power laser parameters and shielding gas on the penetration and microstructure. Another aim in this works was to produce the joint for this thin sheets metal. Penetration depth and microstructure evaluation were emphasized in the analysis. Bead-on-Plate (BOP) and laser lap welding has been conducted on AZ31B with the thickness of 1.0 mm and 0.6 mm for the feasibility study using pulsed wave (PW) fibre laser welding method. Defocusing features was used in order to find the better focal position, which has less occurrence of evaporation (underfill). The effect of different angle of irradiation was also investigated. Two type of shielding gas, Argon (Ar) and Nitrogen (N_2) were used to study the effect of shielding gas. Lastly, the effect of pulsed energy on penetration types and depth of the BOP welded samples was investigated. Microstructure of welded AZ31B thin sheets was studied in this work.

2. **Mechanical and microstructural characterization of single and double pass aluminium AA6061 friction stir weld joints**

(IOP Conference Series: Materials Science and Engineering (2015) pp. 1-8., 100 (012016). ISSN 1757-8981 (Print), 1757-899X (Online)– Scopus Indexed)

Abstract. This study focuses on the effect of single pass (SP), double sided pass (DSP) and normal double pass (NDP) method on friction stir welding of aluminum AA6061. Two pieces of AA6061 alloy with thickness of 6 mm were friction stir welded by using conventional milling machine. The rotational speeds that were used in this study were 800 rpm, 1000 rpm and 1200 rpm, respectively. The welding speed is fixed to 100 mm/min. Microstructure observation of welded area was studied by using optical microscope. Tensile test and Vickers hardness test were used to evaluate the mechanical properties of this specimen. Mechanical property analysis results indicate that at low rotational speeds, defects such as surface lack of fill and tunneling in the welded area can be observed. Vickers hardness of specimens however did not vary much when rotational speed is varied. Welded specimens using single pass method shows higher tensile strength and hardness value compared to both double pass methods up to 180.61 MPa. Moreover, DSP showed better tensile test and hardness test compared to NDP method. The optimum parameters were found to be single pass method with 1200 rpm of rotational speed. Therefore economically sound to only perform SP method to obtain maximum tensile strength for AA6061 FSW with thickness of 6 mm.

3. **The Effect of Taper Pin Ratio on AA7075 Friction Stir Welding**
(Key Engineering Materials, Vol. 701, pp. 154-158, (2016) doi: 10.4028/www.scientific.net/KEM.701.154 - Proceedings)

Abstract This study focuses on the effect of pin taper tool ratio on friction stir welding of aluminum AA7075. Two pieces of AA7075 alloy with thickness of 6 mm were friction stir welded by using conventional milling machine. The shoulder diameter used in this experiment is fix 18mm. The taper pin ratio used are varied at 6:6, 6:5, 6:4, 6:3, 6:2,and 6:1. The rotational speeds that were used in this study were 1000 rpm, 1200 rpm and 1400 rpm, respectively. The welding speeds used are 60 mm/min, 80 mm/min and 100 mm/min. Microstructure observation of welded area was studied by using optical microscope. To evaluate the mechanical properties of this specimen, tensile test was used in this study. Welded specimens using taper pin ratio 6:2 shows higher tensile strength compared to other taper pin ratio up to 197 MPa. Moreover, taper pin ratio 6:1 showed better tensile test compared to taper pin ratio above 6:3. The optimum parameters were found to be taper pin ratio 6:2 with 1000 rpm of rotational speed and 60mm/min welding speed.

4. **Investigation on the effect of Pulsed Energy on strength of Fillet lap Laser welded thin sheet AZ31B magnesium alloy**
(IOP Conference Series: Materials Science and Engineering (2017) doi: 10.1088/1757-899X/238/1/012009 - SCOPUS Indexed)

Abstract AZ31B magnesium alloy have been hugely applied in the aerospace, automotive, and electronic industries. However, welding thin sheet AZ31B was challenging due to its properties which is easily to evaporated especially using conventional fusion welding method such as metal inert gas (MIG). Laser could be applied to weld this metal since it produces lower heat input. The application of fiber laser welding has been widely since this type of laser could produce better welding product especially in the automotive sectors. Low power fiber laser was used to weld this non-ferrous metal where pulse wave (PW) mode was used. Double fillet lap joint was applied to weld as thin as 0.6 mm thick of AZ31B and the effect of pulsed energy on the strength was studied. Bond width, throat length, and penetration depth also was studied related to the pulsed energy which effecting the joint. Higher pulsed energy contributes to the higher fracture load with angle of irradiation lower than 3 º

5. **The mechanical and microstructural study of welded AA7075 using different filler metal**

(International Journal of Computational Methods and Experimental Measurement (2017) doi: 10.2495/CMEM-V5-N5-696-712- SCOPUS Indexed)

Abstract This paper discussed about the consequences of using different filler metal by metal inert gas (MIG) welding process on aluminium alloys Al 7075 sheet metal joint. Nowadays, Al 7075 is widely used in automobile and aviation industry due to its light weight, strong, and high hardness. Fusion welding, such as MIG and TIG were commonly used in joining the aluminium alloys due to its low cost. However, defects usually occurred using fusion welding because of the inaccurate welding parameters and types of filler metal used. The purpose of this study is to determine whether the filler metal with different elements and welding parameters affect the mechanical properties of welded Al 7075. Welding parameters used were current, voltage, welding speed, and Argon (Ar) as shielding gas. Two different types of filler metal were used which is Electrode Rod (ER) 4043 and ER5356 which is from Al-Si and Al-Mg based element, respectively. From microstructure analysis, fusion zone (FZ) of sample welded with ER4043 has a smaller grain size than that of with ER5356. Both filler produced equiaxed den- dritic grain at FZ. Both samples welded with ER4043 and ER5356 has lower hardness value than heat affected zone (HAZ) and base metal (BM) due to the differences in their elements where ER4043 from Al-Si and ER5356 from Al-Mg group. The weld efficiency of sample welded using ER5356 was 61% which was higher compared to sample welded using ER4043 which at 43% and both sample was brittle fractured. Sample welded with ER5356 was fractured at HAZ due to porosity while sample welded with ER4043 fractured at FZ due to the oxide inclusion.

6. **Effects of heat input on mechanical properties of metal inert gas welded 1.6 mm thick galvanized steel sheet**
(IOP Conference Series: Materials Science and Engineering (2011) doi: 10.1088/1757-899X/36/1/012011 - SCOPUS Indexed)

Abstract It is usually a lot easier and less expensive to galvanize steel before it is welded into useful products. Galvanizing afterwards is almost impossible. In this research work, Galvanized Steel was welded by using the ER 308L stainless steel filler material. This work was done to find out an alternative way of welding and investigate the effects of heat input on the mechanical properties of butt welded joints of Galvanized Steel. A 13.7 kW maximum capacity MIG welding machine was used to join 1.6 mm thick sheet of galvanized steel with V groove and no gap between mm. Heat inputs was gradually increased from 21.06 to 25.07 joules/mm in this study. The result shows almost macro defects free welding and with increasing heat input the ultimate tensile strength and welding efficiency decrease. The Vickers hardness also decreases at HAZ with increasing heat input and for each individual specimen; hardness was lowest in heat affected zone (HAZ), intermediate in base metal and maximum in welded zone. The fracture for all specimens was in the heat affected zone while testing in the universal testing machine.

7. **GMA Spot Welding of A7075-T651/AZ31B Dissimilar Alloys Using Stainless Steel Filler**
(Materials and Manufacturing Process (2014) 012118 doi:10.10426914.2014.892614 - ISI paper)

Abstract The aim of this research was to investigate the welding joint's fracture toughness and fracture surface morphologies between A7075-T651 aluminum and AZ31B magnesium dissimilar alloys welded using a new technique of gas metal arc spot lap welding with unconventional ER308L-Si stainless steel filler. The fracture toughness of the welding joints was estimated from yield strength and absorbed charpy impact energy of the joints using Rolfe–Novak–Barsom correlation, and was compared with the fracture toughness of AZ31B parent metal. Fracture surface morphologies were investigated by scanning electron microscopy. The results showed that the joint can achieve a maximum fracture toughness of 93.08% of the AZ31B parent metal. Most of the joints failed at AZ31B alloy, while some failed at A7075-T651 alloy and ER308L-Si nugget. Brittle fracture mechanism was observed for all the joints. It was found that the new gas metal arc spot lap welding technique with ER308L-Si filler could offer very good mechanical properties.